

**A first principle study of structural, electronic
and optical properties of perovskite materials of
KInCl₃ and KGaCl₃**

Roll: 161330

Session: 2016-2017

Report submitted to the Department of Physics at
Jashore University of Science and Technology
In partial fulfillment of the requirements
For the degree of Bachelor of Science
With Honours in Physics

January 2022

Abstract

Perovskite materials KInCl_3 and KGaCl_3 are studied to investigate their properties of use as future solar materials. We present structural, electrical, and optical properties for halide perovskites KInCl_3 and KGaCl_3 . These perovskite compounds has promising electrical and optical characteristics which indicate that they could be used in photovoltaic and other optoelectronic applications. Many properties of condensed matter systems have been studied and successfully described using density functional theory (DFT) based on electronic structure and optical properties calculations. The exchange correlation potential PBE-GGA approach, as implemented in the WIEN2k code, is used to investigate structural optimization, energy band structure, density of states, and optical spectra for these perovskite compounds. The analysis of real and imaginary dielectric tensor components, optical absorption, reflectivity, and refractivity spectra is used to determine the optical performance of the compounds.

Acknowledgement

Firstly, I want to praise the almighty God, the exalted, most gracious and most merciful who enabled me to continue this work and leading towards the fulfillment of the requirements for the degree of Bachelor of Science in Physics

I would like to express my great gratitude to my supervisor Dr. Mohammad Abdur Rashid, for his continuous supervision, constant guidance, enthusiasm, patience and constructive criticisms that provided immense help in preparing this report. I am grateful to him because of the untiring effort and contributions to the development of my work.

Finally, I would like to give my special thanks to my parents for their love, unconditional supporting, blessing, inspiration and co-operation in all step in my life.

Contents

Abstract	i
Acknowledgement	ii
List of Figures	v
List of Abbreviation	vi
1. Introduction	1
2. Basic Quantum Mechanics	4
2.1 Schrödinger groundbreaking equations	4
2.2 Time-independent Schrödinger equation	5
2.3 The wave function	6
2.4 Atoms and molecules	8
2.5 The many-body system and Born-Oppenheimer Approximation	9
2.6 The Hartree-Fock approach	10
2.7 Limitation and failings of the Hartree-Fock approach	12
3. Density Functional Theory (DFT)	14
3.1 Electron Density	15
3.2 Thomas-Fermi Dirac Approximation	15
3.3 The Hohenberg-Kohn Theorems	17
3.3.1. Theorem I	17
3.3.2. Theorem II	18

Contents

3.4 The Kohn-Sham equations	19
3.5 The Exchange-Correlation Functional	21
3.6 Local Density Approximation (LDA)	22
3.7 Generalized-Gradient Approximation (GGA)	23
4. Electronics and Optical Properties of KInCl₃ and KGaCl₃	24
4.1 Crystallographic structure	24
4.2 Band structure	27
4.3 Density of states (DOS)	28
4.4 Optical Properties	29
4.4.1 Dielectric Tensor Components	30
4.4.2 Optical Conductivity	32
4.4.3 Reflectivity Spectra	33
4.4.4 Refractive Index	34
4.4.5 Absorption Coefficient	35
5. Conclusions	37
Bibliography	38

List of Figures

Figure 3.1: Illustration of the self-consistent field (SCF) procedure for solving the Kohn-sham equations.	21
Figure 4.1: Crystal structure for cubic KInCl_3 and KGaCl_3	25
Figure 4.2. Volume optimization curve for (a) KInCl_3 and (b) KGaCl_3	26
Figure.4.3: Band structure for (a) KInCl_3 and (b) KGaCl_3	27
Figure 4.4: The density of state for KInCl_3 and KGaCl_3	29
Figure 4.5: Real dielectric tensor of KInCl_3 and KGaCl_3	30
Figure 4.6: Imaginary dielectric tensor of KInCl_3 and KGaCl_3	31
Figure 4.7: Optical conductivity of KInCl_3 and KGaCl_3	32
Figure 4.8: Optical reflectivity of KInCl_3 and KGaCl_3	33
Figure 4.9: Refractive index of KInCl_3 and KGaCl_3	34
Figure 4.10. Absorption coefficient of KInCl_3 and KGaCl_3	35

List of Abbreviation

BZ	: Brillouin Zone
DFT	: Density Functional Theory
RMT	: Radius Muffin Tin
DOS	: Density of States
GGA	: Generalized Gradient Approximation
PBE	: Perdew-Burke-Ernzerhof
HK	: Hohenberg-Khon
KS	: Khon-Sham
XC	: Exchange correlation
LDA	: Local Density Approximation
TF	: Thomas-Fermi
FP-LAPW	: Full Potential Linear Augmented Plane Wave

**A first principle study of structural, electronic
and optical properties of perovskite materials of
KInCl₃ and KGaCl₃**

Chapter 1

Introduction

The systems name is KInCl_3 and KGaCl_3 and both of these system are perovskite materials. These Perovskites has the cubic crystal structure. Opto-electronic properties of perovskite materials with general formula ‘ ABX_3 ’ (where, A = Monovalent cation, B = Divalent metal cation and X = Anion) has now demonstrated a new horizon for future photovoltaic uses [1, 2]. Metal halide perovskite solar cells have lately risen to prominence as one of the most promising low-cost thin-film photovoltaics contenders (PV). The fundamental understanding of their physicochemical properties is essential for improving their efficiency and stability [3]. The favorable intrinsic properties of these materials including strong absorption coefficient [4] , sharp bandages with low levels of disorder [5], photon recycling capability [6,7] and excellent charge transport characteristics [8], render them as excellent candidates for related optoelectronic applications such as solar cells , light emitting diodes, and transistors [9] . Due to their outstanding optoelectronic capabilities, metal halide perovskites are attracting a lot of attention for a variety of applications. The creation of ecologically benign halide perovskite materials with a variety of crystal structures and compositions opens up previously unimaginable possibilities for achieving desired features and applications [10]. These perovskites have recently emerged as a promising material for low cost and high efficiency solar cells, these perovskite has been used as the replacement for thin-film solar cells [11].

Electronic structure calculations based on density functional theory become more and more popular in condensed matter physics, quantum chemistry and material science. Density functional theory is by far the most widely used approach for electronic structure calculations nowadays. It is usually called first principle method or ab initio method, because it allows people to determine many properties of a condensed matter system by just giving some basic structural information without any adjustable parameter [12]. The accurate approximation for the exchange-correlation functional, which derives from the Kohn-Sham method, is also a major component of DFT [13]. In 1964 Hohenberg and Kohn they proved the electron density, a variable only depending on 3 spatial variables, in principle contains all information about the ground state properties of a system. In atomic and nuclear physics, as well as theoretical chemistry, the Hartree-Fock technique is widely employed [14]. Hartree and Fock solved the complicated and analytically inaccessible many-body Schrödinger equation by deriving a set of self consistent, wave-function based equations that permitted an iterative calculation of energies and other desirable quantities [15].

In 1965, Kohn and Sham constructed a set of self-consistent, iteratively solvable equations, allowing for the first time the implementation of Hohenberg and Kohn's previously exclusively theoretical concept in actual computer simulations [16].

The birth of density functional theory (DFT), which occupies the majority of this project. Kohn was awarded the Nobel Prize in Chemistry in 1998 for his work on the density-functional theory [14]

In our calculations we have used the full-potential linearized augmented plane-wave method (FP-LAPW) as it is implemented in the WIEN2k code. WIEN2k is a software tool that allows you to use density functional theory to calculate the electronic structure of solids (DFT). It uses the full potential (linearized) augmented plane-wave ((L)APW)+local orbitals(lo) approach, which is one of the most accurate methods for calculating band structure. WIEN2k is a multi-featured all-electron system that includes relativistic effects. Within density functional theory, the Linearized Augmented Plane Wave (LAPW) approach has proven to be one of the most accurate ways for computing the electronic structure of solids. WIEN2k is an all electron scheme including relativistic effect and has many features. It is used for computation of structure, electronic and magnetic properties [17].

This report is divided into five chapters. In chapter one, we illustrate the general introduction for perovskite of KInCl_3 and KGaCl_3 . In chapter two, we explain the basic quantum mechanics

such as Schrödinger groundbreaking equations, time-independent Schrödinger equation, the wave function, atoms and molecules, the many-body system and Born-Oppenheimer Approximation, the Hartree-Fock approach, limitation and failings of the Hartree-Fock approach. In chapter three, we discuss the basic density functional theory. It includes electron density, Thomas-Fermi direct approximation, the Hohenberg-Kohn theorems, the Kohn-Sham equations, the exchange-correlation functional, local density approximation (LDA), generalized-gradient approximation (GGA). In chapter four, we discuss our whole calculation system and structure, band structure, density of state (DOS), optical properties of these materials using WIEN2k. In chapter five, we discuss the summary of this working system.

Chapter 2

Basic Quantum Mechanics

Quantum mechanics is an important tool to understand at the theoretical level the electronic structure of chemical compound and the mechanisms, thermodynamics and kinetics of chemical reactions [18]. Quantum mechanics is the study of incredibly small objects. On the scale of atoms and subatomic particles, it explains how matter behaves and interacts with energy. This chapter including the most basic forms valid for many-body systems.

2.1 Schrödinger's groundbreaking equation

Erwin Schrödinger's attempt to describe the so-called 'matter waves' in 1926, where he used de Broglie's relations to describe hypothetical plane waves, led to the most general form of the famous equation named after him, the time-dependent Schrödinger equation [19]

$$i\hbar \frac{\partial}{\partial t} \Psi(\vec{r}, t) = \hat{H}\Psi(\vec{r}, t) \quad (2.1)$$

Where, \hat{H} is the Hamiltonian operator, \hbar is the daric constant and Ψ is the wave function. It is often impracticable to use a complete relativistic formulation of the formula; therefore Schrödinger himself postulated a non-relativistic approximation which is nowadays often used, especially in quantum chemistry.

Using the Hamiltonian for a single particle

$$\hat{H} = \hat{T} + \hat{V} = -\frac{\hbar^2}{2m} \nabla^2 + V(\vec{r}, t) \quad (2.2)$$

Leads to the (non-relativistic) time-dependent single-particle Schrödinger equation

$$i\hbar \frac{\partial}{\partial t} \Psi(\vec{r}, t) = \left[-\frac{\hbar^2}{2m} \nabla^2 + V(\vec{r}, t) \right] \Psi(\vec{r}, t) \quad (2.3)$$

In this project, from now on only non-relativistic cases are considered. For N particles in three dimensions, the Hamiltonian is

$$\begin{aligned} \hat{H} &= \sum_{i=1}^N \frac{\hat{p}_i^2}{2m_i} + V(\vec{r}_1, \vec{r}_2, \dots, \vec{r}_N, t) \\ &= -\frac{\hbar^2}{2} \sum_{i=1}^N \frac{1}{m_i} + V(\vec{r}_1, \vec{r}_2, \dots, \vec{r}_N, t) \end{aligned} \quad (2.4)$$

the corresponding Schrödinger equation reads

$$i\hbar \frac{\partial}{\partial t} \Psi(\vec{r}_1, \vec{r}_2, \dots, \vec{r}_N, t) = \left[-\frac{\hbar^2}{2} \sum_{i=1}^N \frac{1}{m_i} + V(\vec{r}_1, \vec{r}_2, \dots, \vec{r}_N, t) \right] \Psi(\vec{r}_1, \vec{r}_2, \dots, \vec{r}_N, t) \quad (2.5)$$

2.2 Time-independent Schrödinger equation

Special cases are the solutions of the time-independent Schrödinger equation, where the Hamiltonian itself has no time-dependency (which implies a time-independent potential $V(\vec{r}_1, \vec{r}_2, \dots, \vec{r}_N,)$ and the solutions therefore describe standing waves which are called stationary states or orbitals). The time-independent Schrödinger equation is not only easier to treat, but the knowledge of its solutions also provides crucial insight to handle the corresponding time-dependent equation.

The time-independent equation (2.5) is obtained by the approach of separation of variables, i.e. the spatial part of the wave function is separated from the temporal part via [20]

$$\Psi(\vec{r}_1, \vec{r}_2, \dots, \vec{r}_N, t) = \psi(\vec{r}_1, \vec{r}_2, \dots, \vec{r}_N) \tau(t) = \psi(\vec{r}_1, \vec{r}_2, \dots, \vec{r}_N) e^{iEt/\hbar} \quad (2.6)$$

Furthermore, the l.h.s. of the equation reduces to the energy eigenvalue of the Hamiltonian multiplied by the wave function, leading to the general eigenvalue equation

$$E\psi(\vec{r}_1, \vec{r}_2, \dots, \vec{r}_N) = \hat{H} \psi(\vec{r}_1, \vec{r}_2, \dots, \vec{r}_N) \quad (2.7)$$

Again, using the many-body Hamiltonian, the Schrödinger equation becomes

$$E\Psi(\vec{r}_1, \vec{r}_2, \dots, \vec{r}_N) = \left[-\frac{\hbar^2}{2} \sum_{i=1}^N \frac{1}{m_i} + V(\vec{r}_1, \vec{r}_2, \dots, \vec{r}_N, t) \right] \Psi(\vec{r}_1, \vec{r}_2, \dots, \vec{r}_N) \quad (2.8)$$

2.3 The wave function

The term wave function was used several times throughout the presentation. As a result, and in order to better comprehend what follows, a closer examination of the wave function is undertaken.

The first and most important postulate is that the state of a particle is completely described by its (time-dependent) wave function, i.e. the wave function contains all information about the particle's state. The function of wave is a quantity related to moving object, which is represented by the Ψ . The wave function Ψ has no direct physical meaning. The wave function $\Psi(\mathbf{r}, t)$ describes the position of a particle with respect to time. It can be considered as probability amplitude. $|\Psi|^2$ is proportional to the probability of finding a particle at a particular time. It is the probability density.

$$|\Psi|^2 = \Psi^* \Psi$$

The wave function Ψ must be finite everywhere. If Ψ has more than one value at any point, it mean more than one value of probability of finding the particle at that point which is obviously ridiculous. The wave function must be continuous and have a continuous first derivative throughout, as well as being normalizable.

For the sake of simplicity the discussion is restricted to the time-independent wave function. A question always arising with physical quantities is about possible interpretations as well as observations. The Born probability interpretation of the wave function, which is a major principle of the Copenhagen interpretation of quantum mechanics, provides a physical interpretation for the square of the wave function as a probability density [21, 22]

$$P = |\psi(\vec{r}_1, \vec{r}_2, \dots, \vec{r}_N)|^2 d\vec{r}_1 d\vec{r}_2 \dots d\vec{r}_N \quad (2.9)$$

Equation (2.1) describes the probability that particles 1, 2, ..., N are located simultaneously in the corresponding volume element $d\vec{r}_1 d\vec{r}_2 \dots d\vec{r}_N$ [23]. What happens if the positions of two particles are exchanged, must be considered as well. Following merely logical reasoning, the overall probability density cannot depend on such an exchange

$$|\Psi(\vec{r}_1, \vec{r}_2, \dots, \vec{r}_i, \vec{r}_j, \dots, \vec{r}_N)|^2 = |\Psi(\vec{r}_1, \vec{r}_2, \dots, \vec{r}_j, \vec{r}_i, \dots, \vec{r}_N)|^2 \quad (2.10)$$

There are only two possibilities for the behavior of the wave function during a particle exchange. The first one is a symmetrical wave function, which does not change due to such an exchange. This corresponds to bosons (particles with integer or zero spin). The other possibility is an anti-symmetrical wave function, where an exchange of two particles causes a sign change, which corresponds to fermions (particles which half-integer spin) [24, 25].

In this text only electrons are from interest, which are fermions. The antisymmetric fermion wave function leads to the Pauli principle, which states that no two electrons can occupy the same state, whereas state means the orbital and spin parts of the wave function (the term spin coordinates will be discussed later in more detail). The antisymmetric principle can be seen as the quantum-mechanical formalization of Pauli's theoretical ideas in the description of spectra (e.g. alkaline doublets) [26].

Another consequence of the probability interpretation is the normalization of the wave function. If equation (2.9) describes the probability of finding a particle in a volume element, setting the full range of coordinates as volume element must result in a probability of one, i.e. all particles must be found somewhere in space. This corresponds to the normalization condition for the wave function

$$\int d\vec{r}_1 \int d\vec{r}_2 \dots \int d\vec{r}_N |\Psi(\vec{r}_1, \vec{r}_2, \dots, \vec{r}_N)|^2 = 1 \quad (2.11)$$

Equation (2.11) also gives insight on the requirements a wave function must fulfill in order to be physical acceptable. Wave functions must be continuous over the full spatial range and square-integratable [27].

Another very important property of the wave function is that calculating expectation values of operators with a wave function provides the expectation value of the corresponding observable for that wave function [28]. For an observable $O(\vec{r}_1, \vec{r}_2, \dots, \vec{r}_N)$, this can generally be written as

$$O = \langle O \rangle = \int d\vec{r}_1 \int d\vec{r}_2 \dots \int d\vec{r}_N \Psi^*(\vec{r}_1, \vec{r}_2, \dots, \vec{r}_N) \hat{O} \Psi(\vec{r}_1, \vec{r}_2, \dots, \vec{r}_N) \quad (2.12)$$

2.4 Atoms and molecules

All atomic and molecular systems deal with charged particles. The single electron Schrödinger equation where the electron moves in a Coulomb potential, marks a good starting point.

$$i\hbar \frac{\partial}{\partial t} \psi(\vec{r}) = \left[-\frac{\hbar^2}{2m} \vec{\nabla}^2 - \frac{e^2}{4\pi\epsilon_0 |\vec{r}|} \right] \psi(\vec{r}) \quad (2.13)$$

For the sake of simplicity, the so-called atomic units are introduced at this point for subsequent usage. That means the electron mass m_e , the elementary charge e , reduced Planck constant (Diracconstant) \hbar as well as the vacuum permittivity factor $4\pi\epsilon_0$ are all set to unity [29]

The Schrödinger equation for the single electron simplifies to

$$E\psi(\vec{r}) = \left[-\frac{1}{2} \vec{\nabla}^2 - \frac{1}{|\vec{r}|} \right] \psi(\vec{r}) \quad (2.14)$$

This form of the Schrödinger equation is analytically solvable. Although for the description of matter, even atoms, the Schrödinger equation exceeds analytical accessibility soon. Usage of (2.8) allows a construction of a generalized many-body Schrödinger equation for a system composed of N electrons and M nuclei, where external magnetic and electric fields are neglected.

$$E_i \psi_i(\vec{r}_1 \vec{r}_2 \dots \vec{r}_N; \vec{R}_1 \vec{R}_2 \dots \vec{R}_N) = H \psi(\vec{r}_1 \vec{r}_2 \dots \vec{r}_N; \vec{R}_1 \vec{R}_2 \dots \vec{R}_N) \quad (2.15)$$

Equation (2.15) does not seem overly complicated on the first look, but an examination of the corresponding molecular Hamiltonian

$$\hat{H} = -\frac{1}{2} \sum_{i=1}^N \nabla_i^2 - \frac{1}{2} \sum_{k=1}^M \nabla_k^2 - \sum_{i=1}^N \sum_{k=1}^M \frac{Z_k}{r_{ik}} + \sum_{i=1}^N \sum_{j>i}^N \frac{1}{r_{ij}} + \sum_{k=1}^M \sum_{l>k}^M \frac{Z_k Z_l}{R_{kl}} \quad (2.16)$$

Reveals the real complexity of the equation.

In equation (2.16), M_k represents the nuclear mass in atomic units (i.e. in units of the electron mass), Z_k and Z_l represent the atomic numbers, and $r_{ij} = |\vec{r}_i - \vec{r}_j|$, $r_{ik} = |\vec{r}_i - \vec{R}_k|$ and $R_{kl} = |\vec{R}_k - \vec{R}_l|$ represent the distances between electron-electron, electron-nucleus and nucleus-nucleus respectively.

A term-by-term interpretation of the right hand side in (2.16) reveals that the first two terms correspond to the kinetic energies of the electrons and nuclei. The latter three terms denote the

potential part of the Hamiltonian in terms of electrostatic particle-particle interactions. This is reflected by the corresponding signs, where the negative sign denotes an attractive potential between electrons and nuclei, whereas the positive signs denote repulsive potentials between electrons and electrons as well as the nuclei among themselves [23].

2.5 The Many-Body System and Born-Oppenheimer

Approximation

The Hamiltonian of a many-body condensed-matter system consisting of nuclei and electrons can be written as:

$$\hat{H} = -\frac{\hbar^2}{2m_e} \sum_{i=1}^N \nabla_i^2 - \frac{\hbar^2}{2M_k} \sum_{k=1}^M \nabla_k^2 - \sum_{i=1}^N \sum_{k=1}^M \frac{Z_k e^2}{r_{ik}} + \frac{1}{2} \sum_{i=1}^N \sum_{j>i}^N \frac{e^2}{r_{ij}} + \frac{1}{2} \sum_{k=1}^M \sum_{l>k}^M \frac{Z_k Z_l}{R_{kl}} \quad (2.17)$$

The term by term interactions of this equation is described. Taking advantage of the fact, that the mass of a proton is approximately 1800 times larger than the mass of an electron, which is the minimum mass ratio of electron to nucleus (hydrogen atom) and becomes even higher for heavier atoms, another simplification can be introduced. The so called Born-Oppenheimer approximation states that due to the mass difference the nucleus can be, in comparison to the electrons, considered non-moving, i.e. spatially fixed. One can say that the core movement can be neglected [30].

As a consequence, the general Hamiltonian is replaced by the so-called electronic Hamiltonian

$$\hat{H} = -\frac{\hbar^2}{2m_e} \sum_{i=1}^N \nabla_i^2 - \sum_{i=1}^N \sum_{k=1}^M \frac{Z_k e^2}{r_{ik}} + \frac{1}{2} \sum_{i=1}^N \sum_{j>i}^N \frac{e^2}{r_{ij}} \quad (2.18)$$

Or in terms of operators

$$\hat{H}_{el} = \hat{T} + \hat{U} + \hat{V} = \hat{T} + \hat{V}_{tot} \quad (2.19)$$

Especially for problems of molecular physics and quantum chemistry, the electronic Schrödinger equation is of major interest. But despite all simplifications a simple look at equations (2.15) to (2.19) indicates that there are still a few more crucial points left to deal with until a useful solution can be obtained.

Inspection of equations (2.21) and (2.22) shows that the kinetic energy term depend on the nuclear co-ordinates R_{kl} , or in other words, it is only a function of the electron number. Also the electron-electron repulsion \hat{U} is the same for every system with only Coulomb interactions.

Therefore the only part of the electronic Hamiltonian which depends on the atomic molecular system is the external potential \hat{V} caused by the nucleus electron repulsion. Subsequently this also means that \hat{T} and \hat{U} only need the electron number N as input and will therefore be denoted as 'universal', whereas \hat{V} is system-dependent. The expectation value of \hat{V} is also often denoted as the external potential V_{ext} , which is consistent as long as there are no external magnetic or electrical fields [28].

As soon as the external potential is known, the next step is the determination of the wave functions ψ_i which contain all possible information about the system. As simple as that sounds, the exact knowledge of the external potential is not possible for most natural systems, i.e. in similarity to classical mechanics, the largest system which can be solved analytically is a 2-body-system, which corresponds to a hydrogen atom. Using all approximations introduced up to now it is possible to calculate a problem similar to H_2^+ , a single ionized hydrogen molecule. To get results for larger systems, further approximations have to be made.

2.6 The Hartree-Fock Approach

In order to find a suitable strategy to approximate the analytically not accessible solutions of many-body problems, a very useful tool is variational calculus, similar to the least-action principle of classical mechanics. By the use of variational calculus, the ground state wave function ψ_0 , which corresponds to the lowest energy of the system E_0 , can be approached. A useful literature source for the principles of variational calculus has been provided by T. Fließbach [31].

Hence, for now only the electronic Schrödinger equation is of interest, therefore in the following sections we set $\hat{H} \equiv \hat{H}_{el}$, $E \equiv E_{EL}$ and so on.

Observables in quantum mechanics are calculated as the expectation values of operators [10, 11]. The energy as observable corresponds to the Hamilton operator, therefore the energy corresponding to a general Hamiltonian can be calculated as

$$E = \langle \hat{H} \rangle = \int d\vec{r}_1 \int d\vec{r}_2 \dots \int d\vec{r}_N \psi^*(\vec{r}_1, \vec{r}_2, \dots, \vec{r}_N) \hat{H} \psi(\vec{r}_1, \vec{r}_2, \dots, \vec{r}_N) \quad (2.20)$$

The central idea of the Hartree-Fock approach is that the energy obtained by any (normalized) trial wave function, different from the actual ground state wave function, is always an upper bound, i.e. higher than the actual ground state energy. If the trial function happens to be the desired ground state wave function, the energies are equal

$$E_{trial} \geq E_0 \quad (2.21)$$

With

$$E_{trial} = \int d\vec{r}_1 \int d\vec{r}_2 \dots \int d\vec{r}_N \psi_{trial}^*(\vec{r}_1, \vec{r}_2, \dots, \vec{r}_N) \hat{H} \psi_{trial}(\vec{r}_1, \vec{r}_2, \dots, \vec{r}_N) \quad (2.22)$$

And

$$E_0 = \int d\vec{r}_1 \int d\vec{r}_2 \dots \int d\vec{r}_N \psi_0^*(\vec{r}_1, \vec{r}_2, \dots, \vec{r}_N) \hat{H} \psi_0(\vec{r}_1, \vec{r}_2, \dots, \vec{r}_N) \quad (2.23)$$

The expressions above are usually inconvenient to handle. For the sake of a compact notation, in the following the bracket notation of Dirac is introduced. For a detailed description of this notation, the reader is referred to the original publication [32].

In that notation, equations (2.21) to (2.23) are expressed as

$$\langle \psi_{trial} | \hat{H} | \psi_{trial} \rangle = E_{trial} \geq E_0 = \langle \psi_0 | \hat{H} | \psi_0 \rangle \quad (2.24)$$

Proof [11]: The Eigen functions ψ_i of the Hamiltonian \hat{H} (each corresponding to an energy eigenvalue E_i) form a complete basis set, therefore any normalized trial wave function ψ_{trial} can be expressed as linear combination of those Eigen functions.

$$\psi_{trial} = \sum_i \lambda_i \psi_i \quad (2.25)$$

The assumption is made that the Eigen functions are orthogonal and normalized. Hence it is requested that the trial wave function is normalized, it follows that

$$\begin{aligned} \langle \psi_{trial} | \psi_{trial} \rangle &= 1 \\ &= \langle \sum_i \lambda_i \psi_i | \sum_j \lambda_j \psi_j \rangle \\ &= \sum_i \sum_j \lambda_i^* \lambda_j \langle \psi_i | \psi_j \rangle \\ &= \sum_j |\lambda_j|^2 \end{aligned} \quad (2.26)$$

On the other hand, following (2.24) and (2.26)

$$E_{trial} = \langle \psi_{trial} | \hat{H} | \psi_{trial} \rangle = \langle \sum_i \lambda_i \psi_i | \hat{H} | \sum_j \lambda_j \psi_j \rangle = \sum_j E_j |\lambda_j|^2 \quad (2.27)$$

Together with the fact that the ground state energy E_0 is per definition the lowest possible energy, and therefore has the smallest eigenvalue ($E_0 \leq E_i$), it is found that

$$E_{trial} = \sum_j E_j |\lambda_j|^2 \geq E_0 \sum_j |\lambda_j|^2 \quad (2.28)$$

What resembles equation (2.24).

The mathematical framework used above, i.e. rules which assign numerical values to functions, so called functionals, is also one of the main concepts in density functional theory. A function gets a numerical input and generates a numerical output whereas a functional gets a function as input and generates a numerical output [33].

Equations (2.20) to (2.29) also include that a search for the minimal energy value while applied on all allowed N-electron wave-functions will always provide the ground-state wave function (or wave functions, in case of a degenerate ground state where more than one wave function provides the minimum energy). Expressed in terms of functional calculus, where ψ

N addresses all allowed N-electron wave functions, this means [23]

$$\begin{aligned} E_0 &= \min_{\psi \rightarrow N} E[\psi] \\ &= \min_{\psi \rightarrow N} \langle \psi | \hat{H} | \psi \rangle = \min_{\psi \rightarrow N} \langle \psi | \hat{T} + \hat{V} + \hat{U} | \psi \rangle \end{aligned} \quad (2.29)$$

For N-electron systems this search is, due to the large number of possible wave functions on the one hand and limitations in computational power and time, practically impossible. What is possible is the restriction of the search to a smaller subset of possible wave function, as it is done in the Hartree-Fock approximation.

2.7 Limitation and failings of the Hartree-Fock Approach

The number of electrons in an atom or a molecule might be even or odd. The compound is in a single state if the number of electrons is even and they are all in double occupied spatial orbital ϕ_i such system are called closed-shell systems. The number of the electrons is odd as well as compounds with single occupied orbitals and the compounds are in the higher ground state, are called open-shell system. These two types of systems correspond to two different approaches of the Hartree-Fock method. In the restricted HF-method (RHF), all electrons are

considered to be paired in orbitals and other is unrestricted HF-method (UHF), this limitation is lifted totally [34]

The closed shell systems which require the unrestricted approach in order to get proper results. The description of the dislocation of H_2 , where one electron must be located at one hydrogen atom, can logically not be obtain by the uses of the system which places both electrons in the same spatial orbital. The method choosing system is very important point in HF calculation [35].

The scale of the system under investigation might also be a constraint for computations. Khon states a number of $M = p^5$ with $3 \leq p \leq 10$ parameters for a result of the H_2 .

For a system with $N = 100$ electrons the number of parameters rises to

$$M = p^{3N} = 3^{300} \text{ to } 10^{300} \approx 10^{150} \text{ to } 10^{300} \quad (2.30)$$

HF-methods are limited to systems with a small number of involved electrons ($N \approx 10$). The exponential factor in (2.30) this limitation is sometimes called exponential wall. [36]

A many electron wave function cannot be described entirely by a single Slater determinant, the energy obtained by HF calculations is always larger than the exact ground state energy. The Hartree-Fock-limit is the most precise energy obtained using HF-methods. [34]

The difference between E_{HF} and E_{exact} is called correlation energy and can be denoted as [37]

$$E_{corr}^{HF} = E_{min} - E_{HF} \quad (2.31)$$

Despite the fact that E_{corr} usually small against E_{min} , as in the example of a N_2 molecule where

$$E_{corr}^{HF} = 15.9eV < 0.001 \cdot E_{min} \quad (2.32)$$

It has the potential to have a significant impact.

For instance, the experimental dissociation energy of the N_2 molecule is

$$E_{diss} = 9.9eV < E_{corr} \quad (2.33)$$

Which corresponds to a large contribution of correlation energy to relative energies such as reaction energies which are of particular interest in quantum chemistry [38].

Chapter 3

Density Functional Theory

Density Functional Theory (DFT) is a computational quantum mechanical modeling method used in physics, chemistry and material science to investigate the electronic structure of many body system in particular atoms, molecules and the condensed phases. The parameters of various electron systems can be derived using this theory by employing a functional, function of another function, in this case the spatially dependent electron density. As a result of the application of electron density functions, the name density functional theory was coined. The success of the modern DFT method is due to Khon and Sham 1965 idea that the electron kinetic energy be estimated using an extra set of orbitals used to represent the electron density. [39]

DFT's main principle is to describe a many-body interacting system based on its particle density rather than its many-body wave function. Its foundation is the well-known Hohenberg-Khon theorem, which states that all of a systems properties can be considered unique functionals of its ground state density. In many situations, the findings of DFT calculations for condensed pretty well with experimental data, particularly since the 1990s with better approximations for the XC (exchange-correlation) energy functional. Despite advances in DFT, it is still difficult to use it to adequately explain intermolecular interactions, charge transfer excitations, transition states, global potential energy surfaces, and some other strongly correlated system, as well to calculate the band gap of some semiconductors. [40]

3.1 Electron Density

The basic variable of density functional theory, electron density (for N electrons), is defined as [41, 34]

$$n(\vec{r}) = N \sum_{s_1} \int d\vec{x}_2 \dots \int d\vec{x}_N \psi^*(\vec{x}_1, \vec{x}_2, \dots, \vec{x}_N) \psi(\vec{x}_1, \vec{x}_2, \dots, \vec{x}_N) \quad (3.1)$$

It's worth noting that the notation in (3.1) takes into account a wave function with spin and spatial coordinates. The probability of finding a specific electron with any spin in the volume element $d\vec{r}_1$ is given by the integral in the equation. Because electrons are indistinguishable, N times the integral equals the likelihood of finding any electron there. The other electrons represented by the wave function $\psi(\vec{x}_1, \vec{x}_2, \dots, \vec{x}_N)$ have arbitrary spin and spatial coordinates [34].

If the spin coordinates are ignored as well, the electron density can be described as a quantifiable observable that is just reliant on spatial coordinates [41, 36]

$$n(\vec{r}) = N \int d\vec{r}_2 \dots \int d\vec{r}_N \psi^*(\vec{r}_1, \vec{r}_2, \dots, \vec{r}_N) \psi(\vec{r}_1, \vec{r}_2, \dots, \vec{r}_N) \quad (3.2)$$

Before providing a strategy that uses the electron density as a variable, make sure it has all of the essential system information. The total number of electrons can be obtained by integration the electron density over the spatial variables.

$$N = \int d\vec{r} n(\vec{r}) \quad (3.3)$$

What has to be proven is that the electron density uniquely characterizes the external potential, where uniquely means up to an additive constant [34].

3.2 Thomas-Fermi Dirac Approximation

The predecessor to DFT was the Thomas-Fermi (TF) model proposed by Thomas and Fermi in 1927. In this method, they used the electron density $n(r)$ as the basic variable instead of the wave function. The total energy of a system in an external potential $V_{ext}(r)$ is written as a functional of the electron density $n(r)$ as:

$$E_{TF}[n(r)] = A_1 \int n(r)^{\frac{5}{3}} dr + \int n(r) V_{ext}(r) dr + \frac{1}{2} \iint \frac{n(r)n(r')}{|r-r'|} dr dr' \quad (3.4)$$

Where the first term is the kinetic energy of the non-interacting electrons in a homogeneous electron gas (HEG) with $A_1 = \frac{3}{10}(3\pi^2)^{\frac{2}{3}}$ in atomic units ($\hbar = m_e = e = 4\pi/\epsilon_0 = 1$). the kinetic energy density of a HEG is obtained by adding up all of the free-electron energy state $\epsilon_k = \frac{k^2}{2}$ up to the Fermi wave factor $k_F = [3\pi^2 n(r)]^{1/3}$ as:

$$\begin{aligned} t_0[n(r)] &= \frac{2}{2\pi^3} \int_0^{K_F} \frac{k^2}{2} 4\pi K^2 dK \\ &= A_1 n(r)^{5/3} \end{aligned} \quad (3.5)$$

The second term is the classical electrostatic energy of the nucleus-electron Coulomb interaction. The third term is the classical electrostatic Hartree energy approximated by the classical Coulomb repulsion between electrons. In the original TF method, the exchange and correlation among electrons was neglected. In 1930, Dirac extended the Thomas-Fermi method by adding a local exchange term $A_2 \int n(r)^{4/3} dr$ to Eq (3.4) with $A_2 = -\frac{3}{4}(3/\pi)^{1/3}$, which leads Eq. (3.4) to

$$E_{TFD}[n(r)] = A_1 \int n(r)^{\frac{5}{3}} dr + \int n(r) V_{ext}(r) dr + \frac{1}{2} \iint \frac{n(r)n(r')}{|r-r'|} dr dr' + A_2 \int n(r)^{4/3} dr \quad (3.6)$$

The ground state density and energy can be obtained by minimizing the Thomas-Fermi-Dirac equation (3.6) subject to conservation of the total number (N) of electrons. By using the technique of Lagrange multipliers, the solution can be found in the stationary condition:

$$\delta\{E_{TFD}[n(r)] - \mu(\int n(r) dr - N)\} = 0 \quad (3.7)$$

Where μ is a constant known as a Lagrange multiplier, whose physical meaning is the chemical potential (or Fermi energy at T = 0 K). Eq (3.7) leads to the Thomas-Fermi-Dirac equation,

$$\frac{5}{3} A_1 n(r)^{(2/3)} + V_{ext}(r) + \int \frac{n(r')}{|r-r'|} dr' + \frac{4}{3} A_2 n(r)^{(1/3)} - \mu = 0 \quad (3.8)$$

Which can be solved directly to obtain the ground state density. The approximations used in Thomas type approach are so crude that the theory suffers from many problems. The most fundamental flaw is that the theory fails to account for atom-to-atom bonding, preventing molecules and solids from forming. Although it is insufficient to represent electrons in matter, its concept of using electron density as the primary variable demonstrates how DFT work.

3.3 The Hohenberg-Kohn Theorems

Hohenberg and Khon proved DFT to be an accurate theory of many body system in 1964 [40]. The "basic lemma of Hohenberg-Khon" [4] states that not only $n(\vec{r})$ is a functional of $v(\vec{r})$ but that also $v(\vec{r})$ is up to constant determined by $n(\vec{r})$ uniquely [41, 36, 34]. The discussion in this work is limited to non degenerate ground states, following Hohenberg and Khon's original method and proof by reductio ad absurdum [41]. This constraint, however, has no bearing on the offered proof for the second theorem and can be lifted for the first theorem as well [42, 43]. The theory is based upon two theorems.

Theorem-I:

The external potential or the ground state energy E is a unique functional of electron density.

$$E = E[n(r)] \quad (3.9)$$

Where $n(r)$ is the electron density.

Proof:

For the sake of simplicity, I will only analyze the case where the system's ground state is non degenerate. The validity of the theorem can be demonstrated. The proof is based on the notion of minimum energy. Suppose there are two different external potentials $V_{ext}(r)$ and V'_{ext} which differ by more than a constant and lead to the same ground state density $n_0(r)$.

The two external potentials would give two different Hamiltonians, \hat{H} and \hat{H}' which have the same ground state density $n_0(r)$ but would have different ground state wave functions, Ψ and Ψ' , with $\hat{H}\Psi = E_0\Psi$ and $\hat{H}'\Psi' = E'_0\Psi'$. Since Ψ' is not the ground state of \hat{H}' , it follows that

$$\begin{aligned} E_0 &< \langle \Psi' | \hat{H} | \Psi' \rangle \\ &< \langle \Psi' | \hat{H} | \Psi' \rangle + \langle \Psi' | \hat{H} - \hat{H}' | \Psi \rangle \\ &< E'_0 + \int n_0(r) [V_{ext}(r) - V'_{ext}(r)] dr \end{aligned} \quad (3.10)$$

Similarly

$$\begin{aligned} E'_0 &< \langle \Psi | \hat{H}' | \Psi \rangle \\ &< \langle \Psi | \hat{H}' | \Psi \rangle + \langle \Psi | \hat{H}' - \hat{H} | \Psi \rangle \end{aligned}$$

$$< E_0 + \int n_0(r)[V'_{ext}(r) - V_{ext}(r)]dr \quad (3.11)$$

Adding Eq. (3.10) and (3.11) lead to the contradiction

$$E_0 + E'_0 < E_0 + E'_0 \quad (3.12)$$

Hence, no two different external potentials $V_{ext}(r)$ can give rise to the same ground state density $n_0(r)$, i.e., the ground state density determines the external potential $V_{ext}(r)$, except for a constant. That is to say, there is a one-to-one mapping between the ground state density $n_0(r)$, and the external potential $V_{ext}(r)$, although the exact formula is unknown.

Theorem-II

The electron density that minimizes the energy of the overall functional is the true ground state electron density.

$$E[n(r)] \geq E_0[n_0(r)] \quad (3.13)$$

Proof:

The universal functional $F[n(r)]$ can be written as

$$F[n(r)] = T[n(r)] + E_{int}[n(r)] \quad (3.14)$$

Where $T[n(r)]$ is the kinetic energy and $E_{int}[n(r)]$ is the interaction energy of the particles. According to vibrational principle, for any wave function Ψ_0 the energy functional $E[\Psi']$:

$$E[\Psi'] = \langle \Psi' | \hat{T} + \hat{V}_{int} + \hat{V}_{ext} | \Psi' \rangle \quad (3.15)$$

Has its global minimum value only when Ψ' is the ground state wave function Ψ_0 , with the constraint that the total number of the particles is conserved. According to HK theorem I, Ψ' must correspond to a ground state with particle density $n'(r)$ and external potential V'_{ext} , then $E[\Psi']$ is a functional of $n'(r)$ According to variational principle:

$$\begin{aligned} E[\Psi'] &= \langle \Psi' | \hat{T} + \hat{V}_{int} + \hat{V}_{ext} | \Psi' \rangle \\ &= E[n'(r)] \\ &= \int n'(r) V'_{ext}(r) dr + F[n_0(r)] \\ &> E[\Psi_0] \end{aligned}$$

$$\begin{aligned}
&= \int n_0(r)V_{ext}(r)dr + F[n_0(r)] \\
&= E[n_0(r)]
\end{aligned} \tag{3.16}$$

Thus the energy functional $E[n(r)] = \int n(r)V_{ext}(r)dr + F[n(r)]$ evaluated for the correct ground state density $n_0(r)$ is indeed lower than the value of this functional for any other density $n(r)$. Therefore by minimizing the total energy functional of the system with respect to variations in the density $n(r)$, one would find the exact ground state density and energy [40].

3.4 The Kohn-Sham equations

Kohn and Sham introduced an orbital approach for evaluating $F_{ni}[n]$ in 1965, which was a key step toward quantitative modeling of electronic structure. To put it another way, they simply computed the equivalent potential, designated $v_{eff}(r)$, and used it to calculate the kinetic energy of N non-interacting particles given only their density distribution $n(r)$ and used the Schrödinger equation

$$\left(-\frac{\hbar^2}{2M}\nabla^2 + v_{eff}(r) \right) \psi_i(r) = \epsilon_i \psi_i(r) \tag{3.17}$$

Such that $n(r) = \sum_{i=1}^N |\psi_i(r)|^2$ the states ψ_i here are ordered so that the energies ϵ_i are non-decreasing, and the spin index is included in i . If ϵ_N is degenerate with $\epsilon_{(N+1)}$ (and also at finite temperatures), fractional occupations f_i are to be used $n(r) = \sum_{i=1}^{\infty} f_i |\psi_i(r)|^2$, but if only spin-degeneracy is involved, the result for the density is not affected. The kinetic energy is then given by, $F_{ni}[n(r)] = \sum_{i=1}^N \langle \psi_i | \hat{t}_i | \psi_i \rangle = \sum_{i=1}^N \epsilon_i - \int dr n(r) v_{eff}(r)$ where \hat{t}_i is the kinetic energy operator for the i th electron $\hat{T} = \sum_i \hat{t}_i$. The external potential of a system is known in practice, not the density distribution or the effective potential. By calculating a functional derivative of the three-term expression for $F_{HK}[n]$ and rearranging the terms, one may determine the effective potential,

$$v_{eff}(r) = v(r) - e\phi(r) + v_{xc}(r) \tag{3.18}$$

Where we have used Eq. $\frac{\delta F[n]}{\delta n} = -v$ for both the interacting and no interacting system. The electrostatic potential is here

$$\varphi(r) = - \int dr' \frac{n(r')}{|r-r'|} \quad (3.19)$$

And the exchange-correlation potential is defined as

$$v_{xc}(r) = \frac{\delta E_{xc}}{\delta n(r)} \quad (3.20)$$

Given a particular approximation for $E_{xc}[n]$, one obtains $v_{xc}(r)$, and can thus find $v_{eff}(r)$ from $n(r)$ for a given $v(r)$ the set of equations described above is called the Kohn-Sham equations of DFT [44].

Now solving the Kohn-Sham equations. The Kohn-Sham equations have an iterative solution and must be solved in the same way each time. To solve the Kohn-Sham equations for a many-body system, we must first define the Hartree potential and the exchange-correlation potential, as well as the Hartree potential and the exchange-correlation potential, we need to know about the Hartree potential and the exchange-correlation potential, the density of electrons $n(r)$.

Starting with an initial trial electron density, as shown in Figure 3.1, is a well-known method for solving the Kohn-Sham equations. Then, using the trial electron density, calculate these equations.

We will have a set of single electron wave functions after solving the Kohn-Sham equations. We can determine the new electron density using these wave functions. The new electron density is fed into the following cycle as an input. Finally, compare the differences in calculated electron densities for each repetition. The solution of the Kohn-Sham equations is considered to be self-consistent if the difference in electron density between consecutive iterations is less than a properly specified convergence threshold. The estimated electron density is now the ground state electron density, and it can be used to calculate the system's total energy [45].

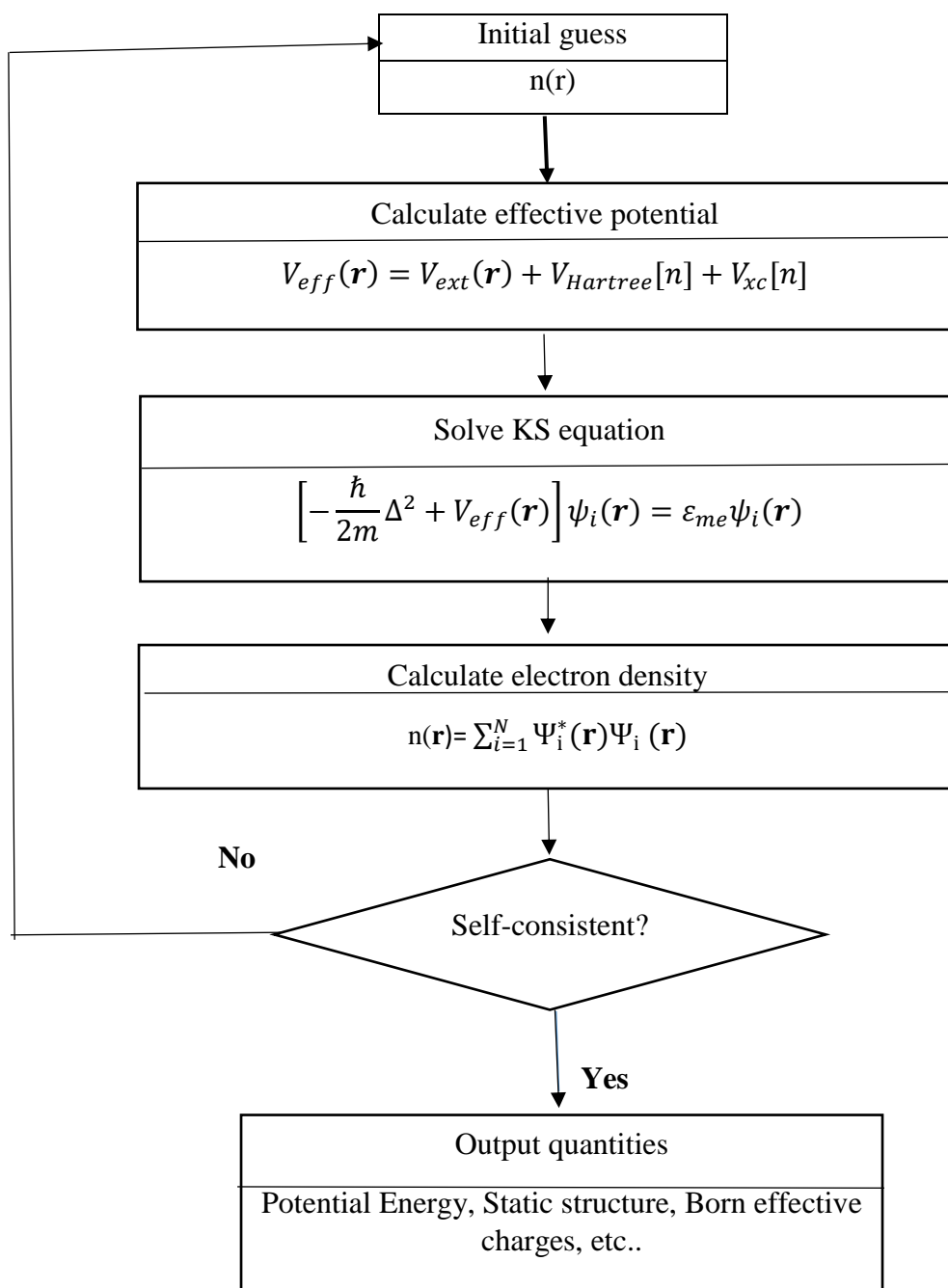


Figure 3.1: Illustration of the self-consistent field (SCF) procedure for solving the Kohn-Sham equations.

3.5 The Exchange-Correlation Functionals

The true shape of the exchange-correlation functional is unknown, which makes solving the Kohn-Sham equations difficult. To approximate the exchange-correlation functional, two main

approximation methods have been implemented. In DFT calculations, the local density approximation (LDA) is the first attempt to estimate the exchange-correlation functional. The generalized gradient approximation is the second well-known class of approximations to the Kohn-Sham exchange-correlation functional (GGA). The local electron density and the local gradient in the electron density are included in the exchange and correlation energies in the GGA approximation [45].

3.6 Local Density Approximation (LDA)

The simplest approximation to the exchange-correlation functional is the local density approximation (LDA).

The local density approximation is based on the assumption that the energy density of a homogeneous electron gas with the same electron density r at every location in the molecule has the value that would be supplied by a homogeneous electron gas with the same electron density r at that point. The word "local" was coined to distinguish the approach from those in which the functional is dependent not only on r but also on the gradient (first derivative) of r , the difference deriving from the assumption that a derivative is a nonlocal characteristic. LDA functional have been mainly supplanted by local spin density approximation (LSDA; see below) functional, which are an extension of the approach [46].

As a practical approximate expression for $E_{xc}[n]$, Kohn and Sham suggested what is known in the context of DFT as the local density approximation, or LDA:

$$E_{xc}[n(r)] \simeq \int dr n(r) \epsilon_{xc}(n(r)) \quad (3.21)$$

Where $\epsilon_{xc}(n)$ is the exchange correlation energy per electron in a uniform electron gas of density n . this quantity is known exactly in the limit of high density, and can be computed accurately at densities of interest, using Monte Carlo techniques.

Note that the only difference between the resulting computational scheme and a naive mean field approach is the addition of the potential

$$v_{xc}(r) = \frac{d(n\epsilon_{xc}(n))}{dn} \quad (3.22)$$

To the electrostatic potential at the appropriate step in the self-consistency loop. The corresponding expression for the ground state energy is:

$$E_0 = \sum_{i=1}^N \epsilon_i - E_{es}[n(r)] + \int dr n(r)(\epsilon_{xc}(n(r)) - v_{xc}(n(r))) \quad (3.23)$$

Where the first term is the no interacting energy, the second term subtracts half of the double counting of the electrostatic energy as in the Hartree scheme, and the last term is a similar subtraction for the exchange correlation energy [47].

The local approximation is only valid in a purely theoretical sense when the density is slowly changing. Despite the fact that atom and molecule densities are typically highly inhomogeneous, LDA produces remarkably good results. For equilibrium structures, harmonic frequencies, and dipole moments in molecules, LDA has been found to yield reasonably satisfactory results [48].

3.7 Generalized-Gradient Approximation (GGA)

The development of various generalized-gradient approximations (GGAs) which include density gradient corrections and higher spatial derivatives of the electron density and give better results than LDA in many cases. Three most widely used GGAs are the forms proposed by Becke (B88), Perdew et al and Perdew, Burke and Enzerhof (PBE). . The definition of the XC energy functional of GGA is the generalized form of LSDA to include corrections from density gradient $n(r)$ as

$$\begin{aligned} E_{XC}^{GGA}[n_{\uparrow}(r), n_{\downarrow}(r)] &= \int n(r) \epsilon_{XC}^{hom}(n_{\uparrow}(r), n_{\downarrow}(r), |\nabla n_{\uparrow}(r)|, |\nabla n_{\downarrow}(r)|, \dots) dr \\ &= \int n(r) \epsilon_{XC}^{hom}(n(r)) F_{XC}(n_{\uparrow}(r), n_{\downarrow}(r), |\nabla n_{\uparrow}(r)|, |\nabla n_{\downarrow}(r)|, \dots) dr \end{aligned} \quad (3.24)$$

Where F_{XC} is dimensionless and $\epsilon_X^{hom}(n(r))$ is the exchange energy density of the unpolarized HEG. F_{XC} Can be decomposed linearly into exchange contribution F_X and correlation contribution F_C as $F_{XC} = F_X + F_C$. For a detailed treatment of F_X and F_C in different GGAs.

In general, GGA outperforms LDA in predicting molecular bond length and binding energy, crystal lattice constants, and other properties, especially in systems with rapidly fluctuating charge density. However, in ionic crystals, GGA overcorrects LDA results when the lattice constants from LDA calculations match experimental data well, but GGA overestimates it [40].

Chapter 4

Electronic and Optical Properties of KInCl_3 and KGaCl_3

4.1 Crystallographic structure

The KInCl_3 and KGaCl_3 structure is cubic. The space group for both of these structure is pm-3m (no. 221). Obtained optimized lattice parameters along the available theoretical parameters and Wyckoff positions are collected in table.

Table: Optimized lattice parameters and Wyckoff positions for cubic KInCl_3 and KGaCl_3

Perovskite compounds	Optimized Lattice Parameters (\AA)	Wyckoff positions			
		Atom	x	y	z
KInCl_3	5.4320	K	0	0	0
		In	0.5	0.5	0.5
		Cl	0.5	0.5	0
KGaCl_3	5.1428	K	0	0	0
		Ga	0.5	0.5	0.5
		Cl	0.5	0.5	0

Optimized lattice parameters for KInCl_3 and KGaCl_3 are in closed with the available theoretical parameters. These parameters are then used to compute the desired properties of the materials being studied. The value of $(\alpha, \beta, \gamma = 90^\circ)$ for these compounds. The muffin tin radii (RMT) $=2.3$. Where the value of $RK_{max} = 8.5$ (R is the atomic radii and K_{max} gives the plane wave cut-off). Energy converging criteria $= 0.0001$ Ry and a separation with cut-off energy (e_{cut}) $= -0.6Ry$ between core state and valance state and the number of k points 1000. Fig.4.1 shows the crystal structure for these two compounds.

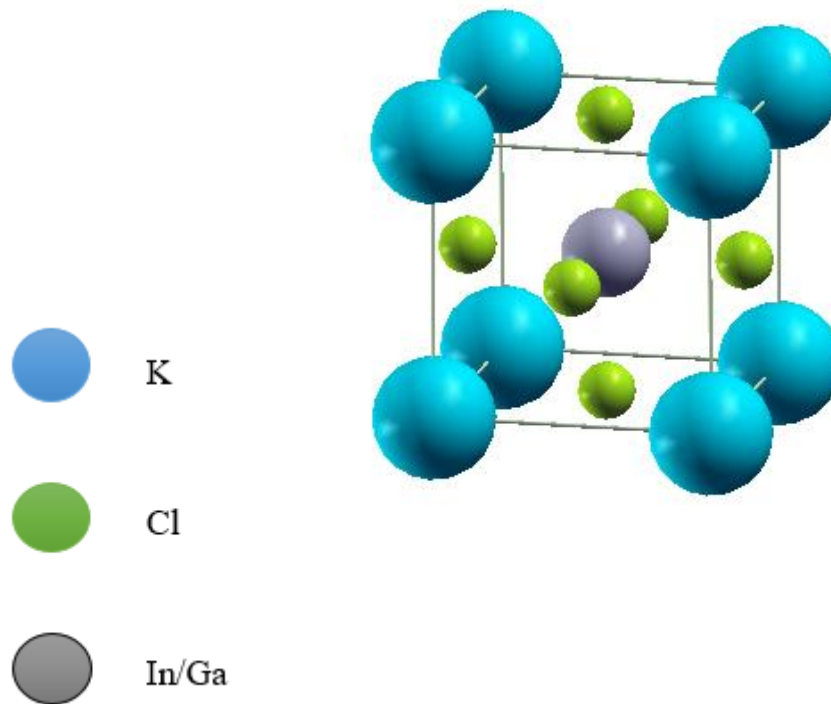


Figure 4.1: Crystal structure for cubic KInCl_3 and KGaCl_3 .

From these structure we see that K atoms are present at corner position, I n/Ga atoms are in center position and Cl atoms are in the middle position. Crystalline structures are drawn by using the XCrySDen software and have optimized structures using the PBE-GGA approximation. Optimized lattice parameter are used to determine the volume optimization curve for minimum energy state. .Firstly, energy v/s volume optimization calculation is performed for both of these studied compounds. Energy v/s volume optimization curve are plotted for these compounds are presented in Figure. 4.2 (a, b) [48].

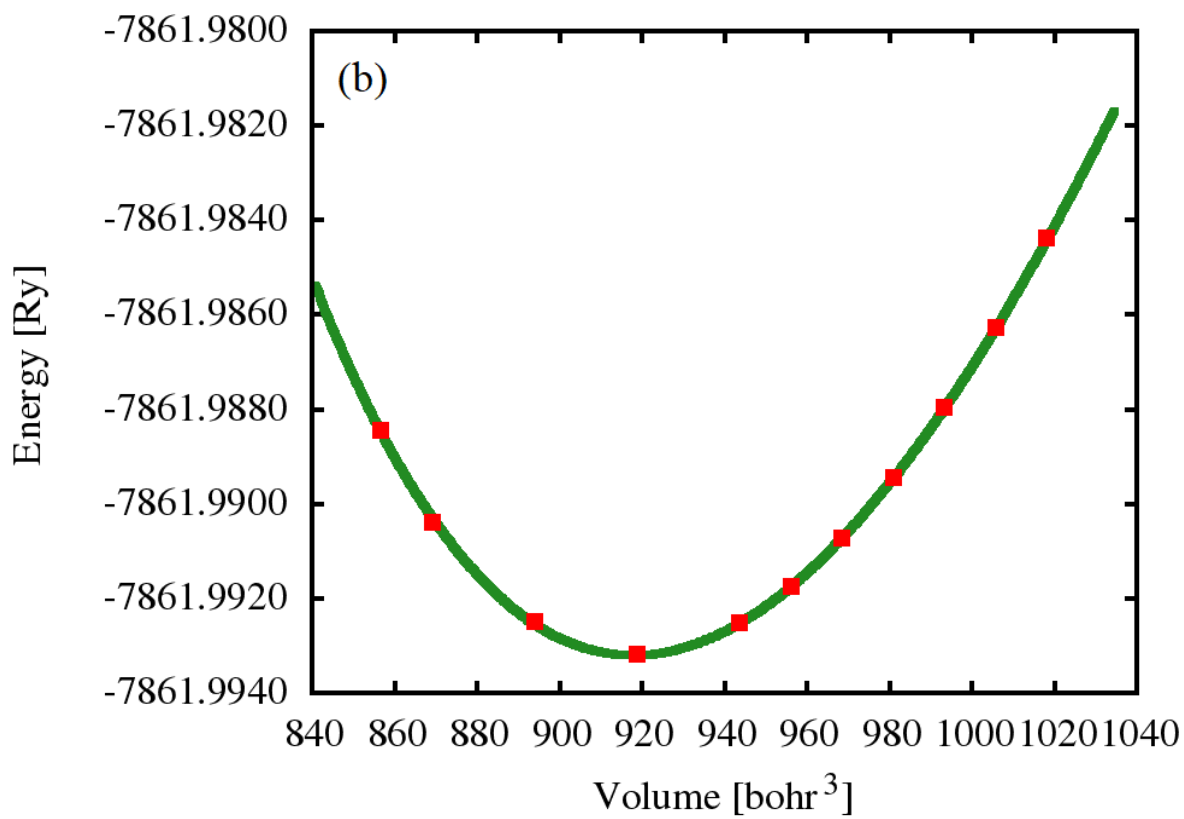
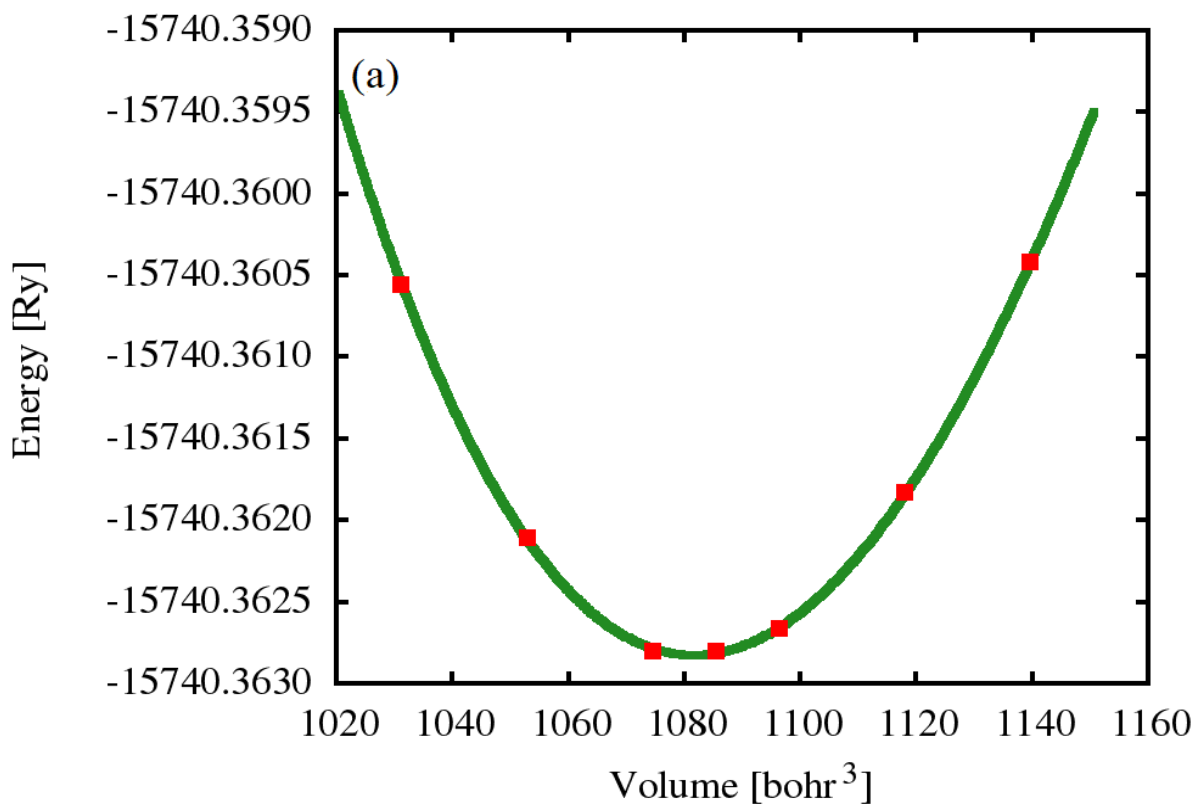


Figure 4.2. Volume optimization curve for (a) KInCl_3 and (b) KGaCl_3

4.2 Band structure

The quantum-mechanical behavior of electrons in solids is described by a theory or band structure. We discuss the electronic properties of band structure for the two compounds of KInCl_3 and KGaCl_3 . The band structure calculation were performed within PBE-GGA along with high symmetry direction of Brillouin Zone. To compute the structural parameters for indium and gallium based perovskite materials of KInCl_3 and KGaCl_3 , we using the most accurate exchange and correlation functional. The energy measure scale in eV . The calculated electronic band structure of these compounds KInCl_3 and KGaCl_3 as shown in Figure 4.3. (a, b).

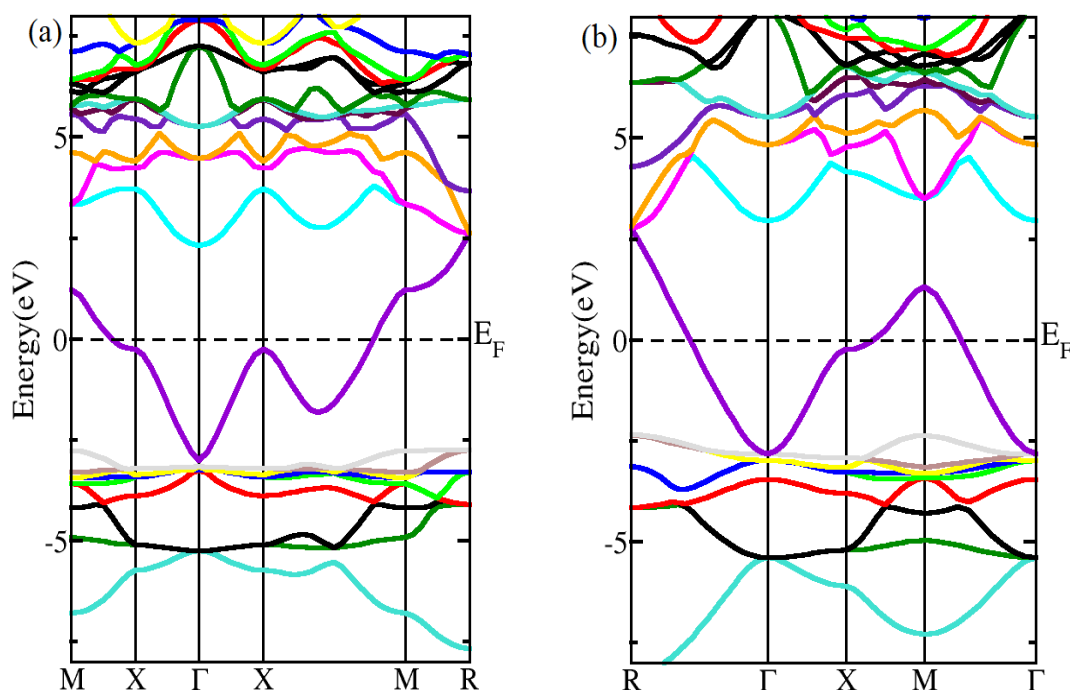


Figure.4.3: Band structure for (a) KInCl_3 and (b) KGaCl_3

From this calculations to identify the energy band gap, energy band structure and electronic response for both of these materials. From this figure.3 (a, b) we see that conduction band enter into the valance band across the fermi level, so there is no band gap in the fermi level. Generally we found band gap in semiconductors and insulators. Since the zero band gap and metallic type

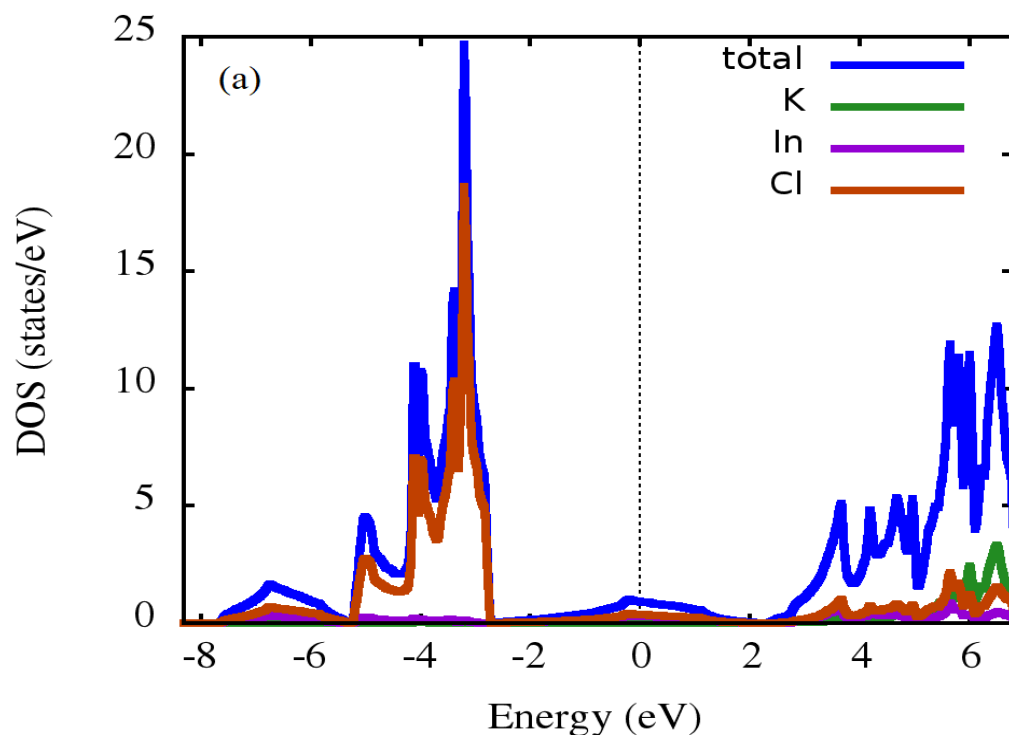
so these materials can be used to produce electrical wire and other electrical devices. From this behavior we say that, both of this compounds are metallic types [49, 50].

4.3 Density of states (DOS)

To better understand the electrical characteristics of KInCl_3 and KGaCl_3 perovskite materials, the total density of state has been examined. The first step in determining a possible electrode material's electronic properties is to establish whether it is metallic, semiconducting, or insulating. The energy band gaps between valance and conduction bands can be deduced from the calculated density of states [51].

The band gaps, or the energy difference between the top of the valence band and the bottom of the conduction band, can be read using the DOS charts. The primary quantities that govern the electronic structure of a system are the energy band structure and the corresponding density of states. Their inspection provides information about the electric property (metal, insulator or semiconductor) and gives insight into the chemical bonding [17].

The density of state (DOS) that describes the electron distribution in the energy spectrum is shown in Figure.4.4: (a, b)



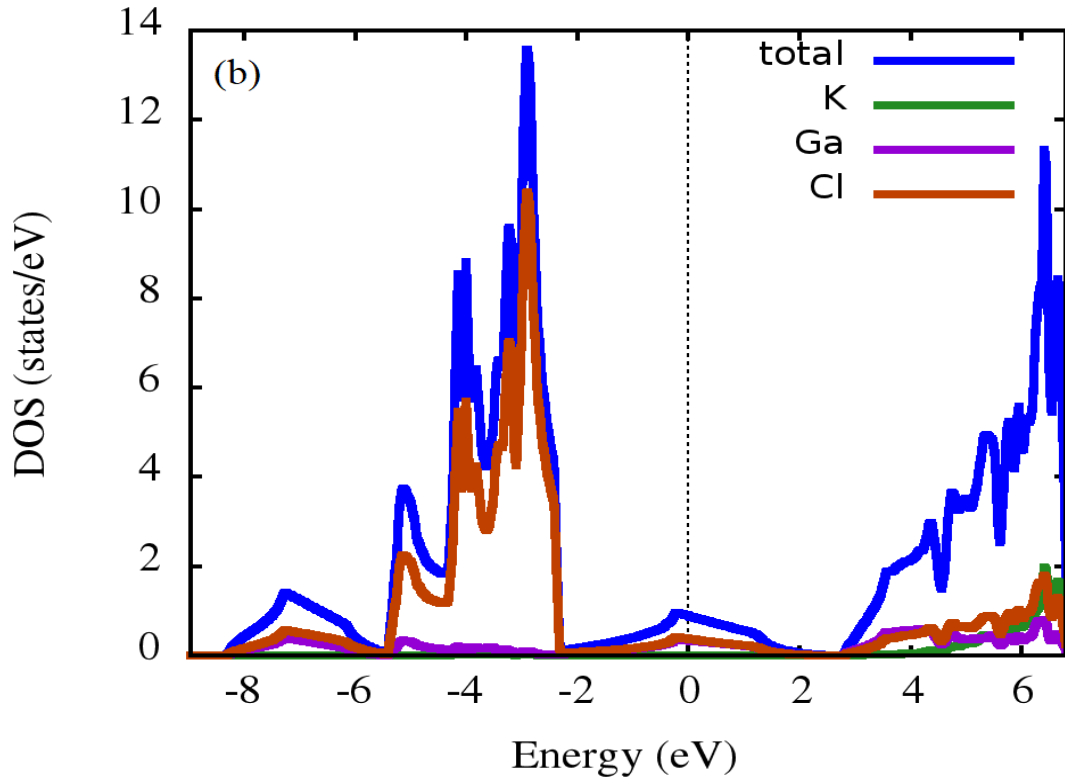


Figure .4.4: The density of state for KInCl_3 and KGaCl_3

The electronic state is separated into three regions: lower valence band (LVB), upper valence band (UVB), and conduction band (CB) [52]. In Fig.4.4 (a) we see that in the valence band the contribution of Cl is higher than the In and K but the very little amount K is contributed in the valence band. In the conduction band K is contributed than the others. In Fig.4.4 (b) we see that the Cl is more contributed in the valence band than the Ga and K. But the conduction band the Cl and K is overlapping and is more contributed than the Ga.

The DOS is calculated using the linear analytic tetrahedron method to evaluate the integrals over the constant energy surfaces. In our calculation, we used a mesh of 1000 k-point in the first Brillouin zone [53].

4.4 Optical properties of KInCl_3 and KGaCl_3

The optical characteristics of perovskite compounds have been studied in order to show they could be used in various optoelectronic applications. The energy gap computed using PBE-GGA for all the studied compounds are in better reconciliation with earlier reported theoretical

data, computations for comprehensive optical properties such as, real and imaginary dielectric tensor components, absorption coefficient, and reflectivity and refractivity spectra are performed using the PBE-GGA method. For optical properties calculation, using plasma frequency are 2.981 and 3.153 for both of these perovskite KInCl_3 and KGaCl_3 .

4.4.1 Dielectric tensor components $\varepsilon(\omega)$

The optical impedance of medium during electromagnetic interaction is investigated using the frequency dependent complex dielectric function $\varepsilon(\omega)$. The complex dielectric function is represented as:

$$\varepsilon_{\alpha\beta}(\omega) = \varepsilon_1(\omega) + i\varepsilon_2(\omega)$$

Here, $\varepsilon_1(\omega)$ and $\varepsilon_2(\omega)$ are the real and imaginary components of dielectric tensor, which they are combined and produced the dielectric tensor $\varepsilon(\omega)$. Where, $\varepsilon(\omega)$ indicates the amount of energy stored in any medium and the energy loss during absorption of sunlight, respectively.

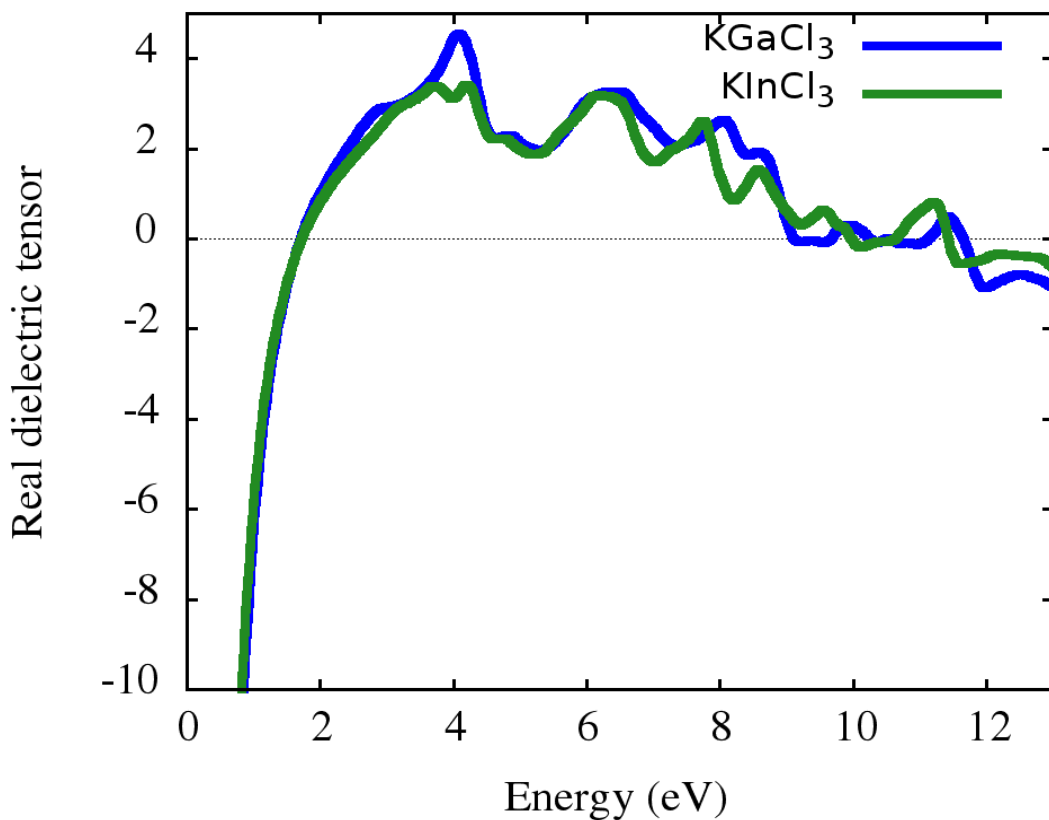


Figure. 4.5: Real dielectric tensor of KInCl_3 and KGaCl_3

The Dielectric Constant is a measurement of a substance's capacity to store electrical energy in an electric field. Both of the real and imaginary dielectric tensor for KInCl_3 and KGaCl_3 obtained from PBE-GGA potential. Mathematically, real and imaginary dielectric tensor components are represented.

For real dielectric tensor, we see that the curve is started 0.9 eV energy. Where the curve is increasing above and creating the large peak point for KGaCl_3 at 4 eV energy. After 4 eV energy the curve is decreasing with increasing energy. The most essential parameter in the real section of the dielectric tensor is the static constant at 0 eV energy, which is dependent on the material's energy gap and has an inverse relationship with it.

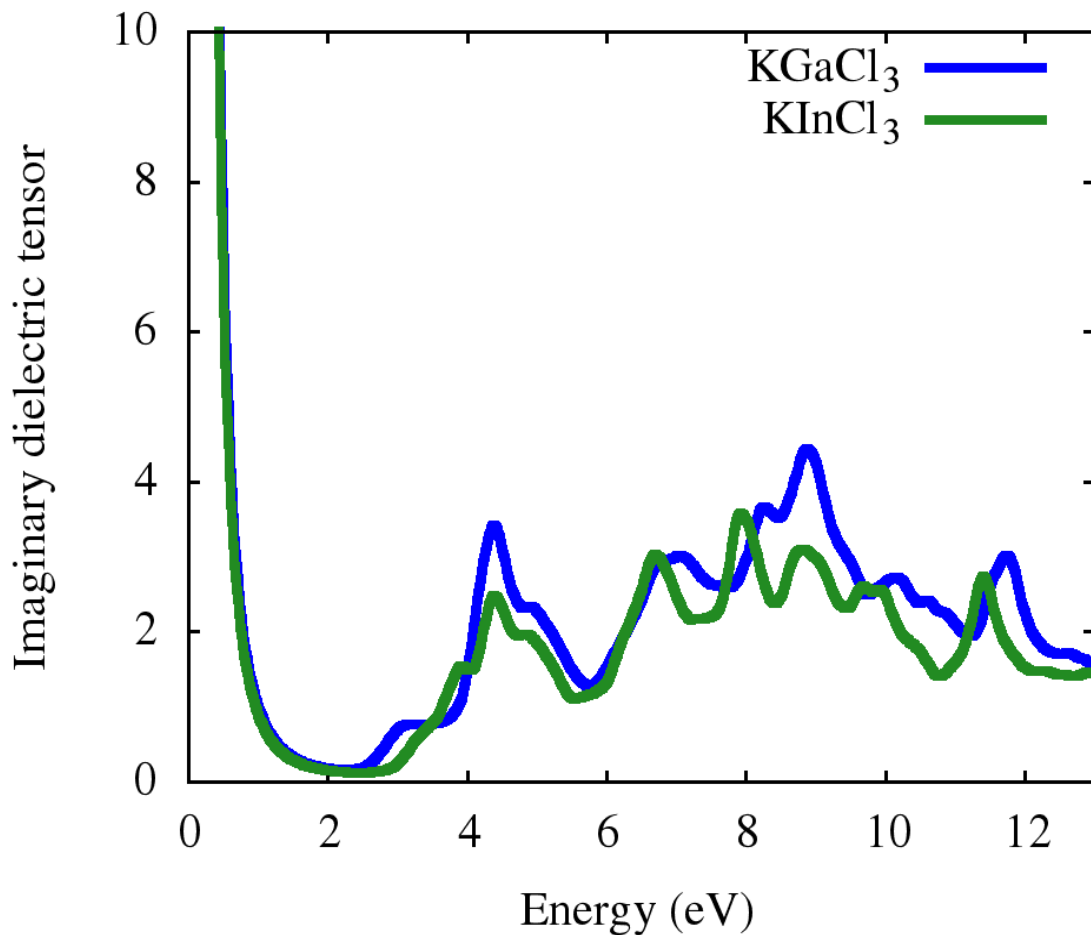


Figure .4.6: Imaginary dielectric tensor of KInCl_3 and KGaCl_3

Electronic transitions causes the distinct peaks in the imaginary dielectric tensor, which can be explained by inter-band transitions between the valence and conduction bands. Peak positions

and likely dominant transitions for all of the perovskite compounds investigated. In these figure. The imaginary curve for both of these materials is decreases directly and at the 2 eV energy the value is zero. After 2 eV energy the curve is increasing with energy and creating the pack position. Where the high peak point creating at the 9 eV energy [54].

4.4.2 Optical conductivity $\sigma(\omega)$

The ability of a medium to generate a conduction phenomenon as electromagnetic radiations try to propagate through it is determined by optical conductivity. As electronic conduction is a matter of putting electrons in the conduction band, one other way to achieve this goal is to give an electron bound to the atoms enough energy to break the bond and set it free to move. The optical conductivity is shown in figure. 4.7. In these figure shows that firstly the conductivity is decreases and at the 2 eV energy the conductivity after 2 eV energy the curve is increasing with increasing energy. These curves are the maximum value of the optical conductivity at 9 eV for the KGaCl_3 compound. So the KGaCl_3 has more conductivity than the KInCl_3 . Where the energy range (0-12) eV [55].

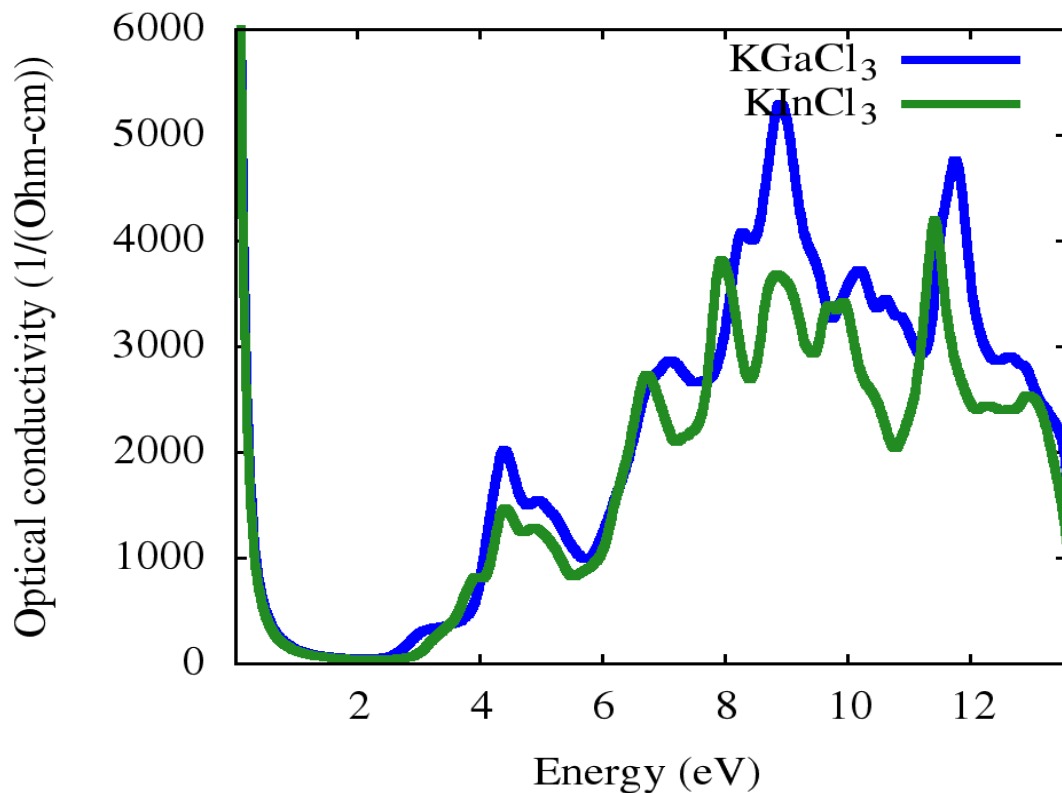


Figure.4.7 Optical conductivity of KInCl_3 and KGaCl_3

4.4.3 Reflectivity spectra $R(\omega)$

This is a measurement of a surface's ability to reflect radiation; it is equivalent to the reflectance of a sufficiently thick layer of material for the reflectance to be thickness independent. Any compound's potential as a perfect absorber is entirely dependent on its reflectance and reflectivity spectra. The reflectivity of light from a surface depends upon the angle of incidence and the plane of polarization of the light. The normal incidence reflectivity is dependent upon the indices of refraction of the two media. Optical response both of these materials can also be explained in term of frequency dependent optical reflectivity $R(\omega)$ is shown in figure 4.8. In this figure the optical reflectivity is zero at the 2 eV energy. From the 2 eV energy the curve is increasing above with increasing the energy. From both of these curve we get KGaCl_3 has large optical reflectivity [56].

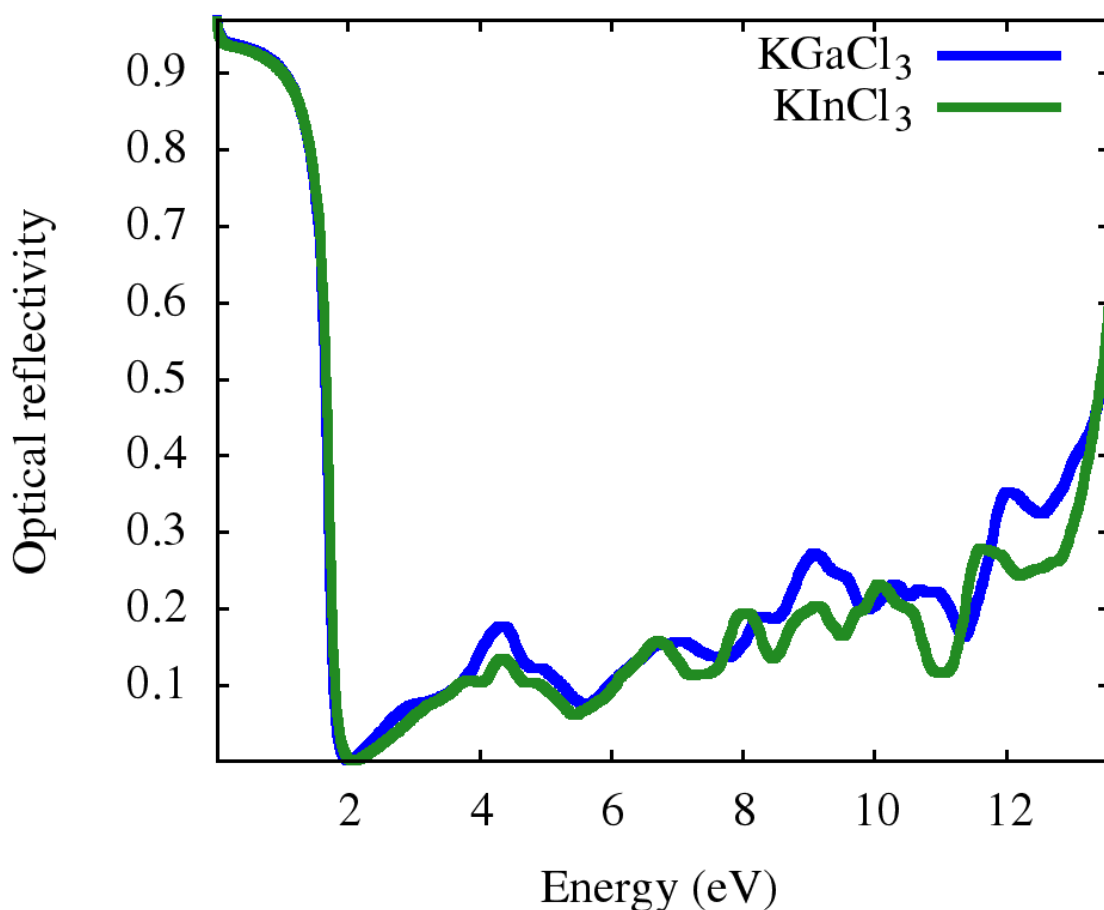


Fig 4.8. Optical reflectivity of KInCl_3 and KGaCl_3

4.4.4 Refractive index $\eta(\omega)$

The refractive index is calculated by dividing the speed of light in a vacuum by the speed of light in a second medium with a higher density (also known as the Index of Refraction). The most common symbol for the refractive index variable is the letter 'n'. The higher the refractive index of a substance, the greater the deflection (or refraction) of a light beam entering or exiting it. The refractive index, as we all know, refers to how quickly light travels through certain materials. The refractive index of the materials varies with the frequency. The refractive index tends to decrease, with increasing frequency. Refractive index of perovskites materials help in selecting proper materials for solar cell, solid-state lighting and lasing applications. In this figure the refractive curve is decreases downward and before 2 eV energy the curve is increasing up and give the large peak at 4 eV energy for KGaCl_3 . After this energy level the curve is decrease at the bottom. The refraction index with energy is plotted in Fig. 4.9 [57].

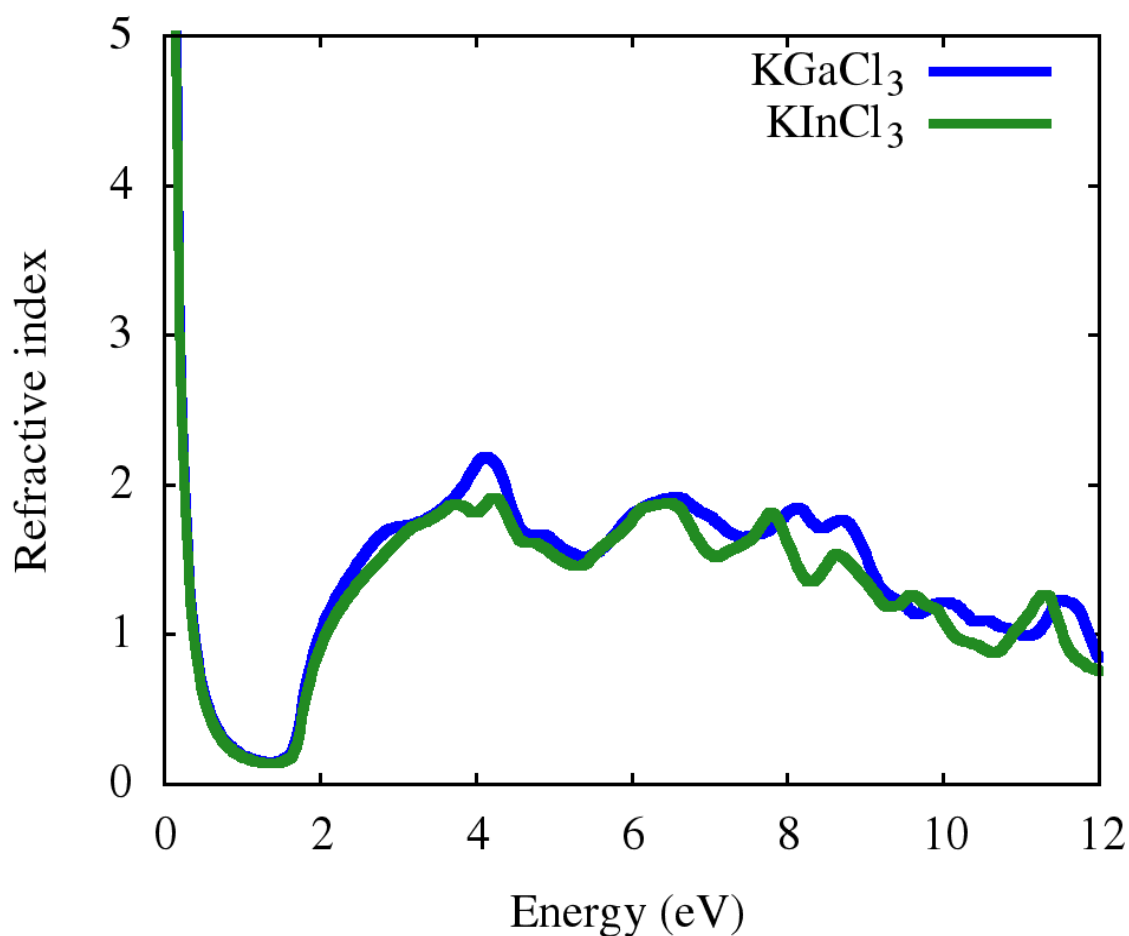


Figure 4.9: Refractive index of KInCl_3 and KGaCl_3

4.4.5 Absorption coefficient $\alpha(\omega)$

The absorption coefficient specifies how far light of a specific wavelength can reach into a substance before being absorbed. Light is only badly absorbed in a material with a low absorption coefficient, therefore if the substance is thin enough, it appears transparent to that wavelength. The wavelength of the absorbed light, as well as the substance, determine the absorption coefficient. Metal conductors have a high absorption coefficient in general. Semiconductors have a sharp edge in their absorption coefficient because light with energy below the band gap does not have enough energy to push an electron from the valence band into the conduction band. As a result, none of this light is absorbed. For photons with energy above the band gap, the absorption coefficient is not constant, but it is still highly dependent on wavelength. The probability of absorbing a photon is proportional to the possibility of a photon and an electron interacting in a way that causes them to move from one energy band to the next [58].

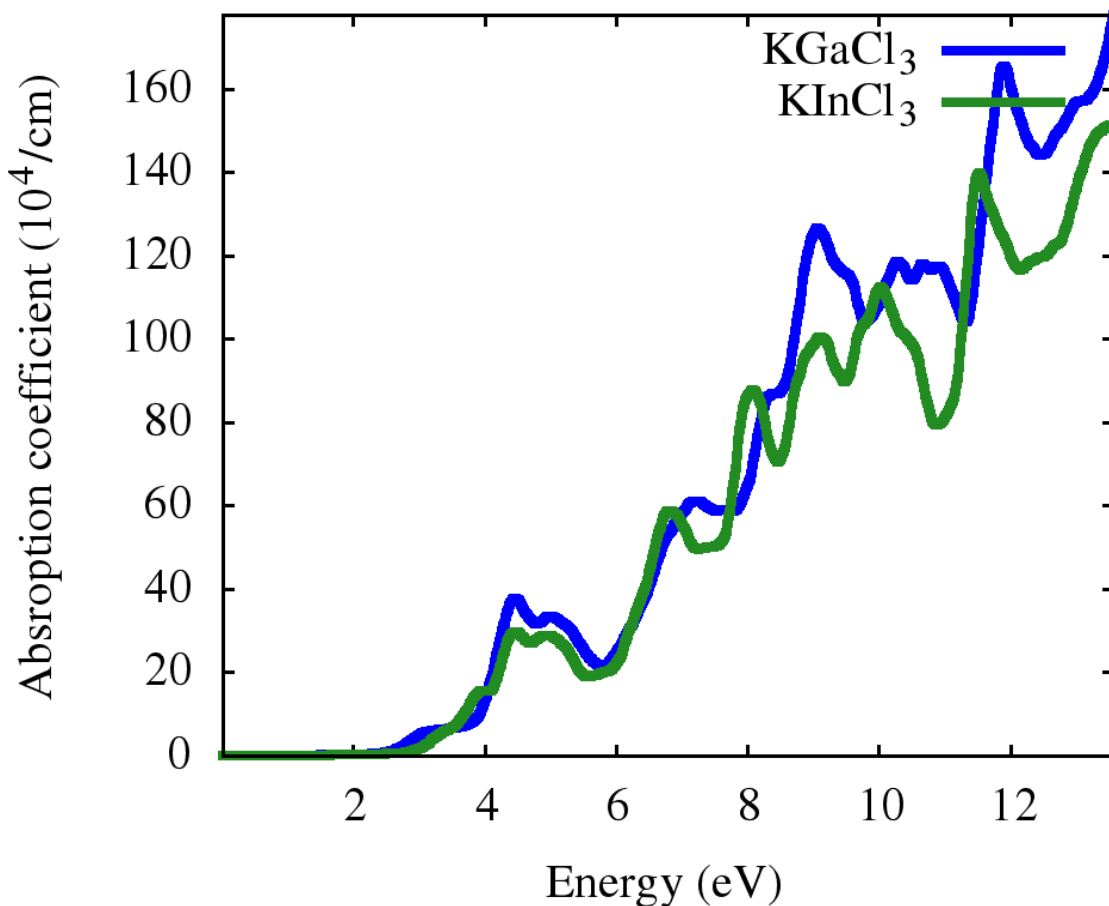


Fig 4.10. Absorption coefficient of KInCl_3 and KGaCl_3

The absorption coefficient, α is related to the extinction coefficient, k by the following formula

$$\alpha = \frac{4\pi k}{\lambda}$$

This equation is the absorption coefficient equation. Where λ is the wavelength. Absorption coefficient computed for KInCl_3 and KGaCl_3 compounds are presented in figure 4.10.

Fig 4.10 shows that the absorption curves are continuously increasing with energy (eV) level to the above on from after 2 eV energy. The visible light range is (1.8-3.1) eV. In this figure the two curve values are zero at the visible light range so that is means that both of these material cannot absorbed the visible light. So both of this materials are good absorber and good conductor the KGaCl_3 curve has much absorption coefficient than the KInCl_3 curve. [58, 59].

Conclusions

We have performed first principles calculation to investigate the electronic and optical properties of perovskite KInCl_3 and KGaCl_3 . In our calculation, we have used density functional investigations for halide perovskite of KInCl_3 and KGaCl_3 which are performed by using the full potential linearized augmented plane wave (FP-LAPW) method and PBE-GGA method as embodied in WIEN2k code. Then the electronic properties of the optimized state were analyzed such as band gap energy, the density of states (DOS). The optical properties such as real and imaginary dielectric tensor, reflectivity, optical conductivity, refractive index and absorption coefficient. Using lattice parameters we find the crystal structure. We calculate the band structure and the total density of state and shows that below the Fermi level. In the band structure there is no band gap, where the conduction band enter into the valance band across the Fermi level. These perovskite materials are metallic types. Absorption spectra and enhanced integrated absorption coefficient (IAC) recorded. Perovskite materials are effective which utilize in future photovoltaic applications.

Bibliography

- [1] K.A. Parrey, T. Farooq, S.A. Khan, U. Farooq, A. Gupta, *Computational Condensed Matter* 16(1 – 8) (2019), e00381.
- [2] Y. Li, X. Gong, P. Zhang, X. Shao, *Chem. Phys. Lett.* 716 (2019) 76–82.
- [3] Yang, W. S.; Park, B. W.; Jung, E. H.; Jeon, N. J.; Kim, Y. C.; Lee, D. U.; Shin, S. S.; Seo, J.; Kim, E. K.; Noh, J. H.; et al. Iodide Management in Formamidinium-LeadHalide-Based Perovskite Layers for Efficient Solar Cells. *Science* 2017, 356 (6345), 1376–1379.
- [4] Yang, W. S.; Noh, J. H.; Jeon, N. J.; Kim, Y. C.; Ryu, S.; Seo, J.; Seok, S. Il. HighPerformance Photovoltaic Perovskite Layers Fabricated through Intramolecular Exchange. *Science* 2015, 348 (6240), 1234–1237.
- [5] Sadhanala, A.; Deschler, F.; Thomas, T. H.; Dutton, S. E.; Goedel, K. C.; Hanusch, F. C.; Lai, M. L.; Steiner, U.; Bein, T.; Docampo, P.; et al. Preparation of Single Phase Films of $\text{CH}_3\text{NH}_3\text{Pb}(\text{I}_{1-x}\text{Br}_x)_3$ with Sharp Optical Band Edges. *J. Phys. Chem. Lett.* 2014, 5 (15), 2501-2505.
- [6] Pazos-Outon, L. M.; Szumilo, M.; Lamboll, R.; Richter, J. M.; Crespo-Quesada, M.; Abdi-Jalebi, M.; Beeson, H. J.; Vru ini, M.; Alsari, M.; Snaith, H. J.; et al. Photon Recycling in Lead Iodide Perovskite Solar Cells. *Science* 2016, 351 (6280), 1430– 1433.
- [7] Richter, J. M.; Abdi-Jalebi, M.; Sadhanala, A.; Tabachnyk, M.; Rivett, J. P. H.; m PazosOutón L. M.; Gödel, K. C.; Price, M.; Deschler, F.; Friend, R. H. Enhancing

Photoluminescence Yields in Lead Halide Perovskites Perovskites by Photon Recycling
And Light Out-Coupling. *Nat. Commun.* 2016, 7, 13941

- [8] Stranks, S. D.; Eperon, G. E.; Grancini, G.; Menelaou, C.; Alcocer, M. J. P.; Leijtens, T.; Herz, L. M.; Petrozza, A.; Snaith, H. J. Electron-Hole Diffusion Lengths Exceeding 1 Micrometer in an Organometal Trihalide Perovskite Absorber. *Science* 2013, 342 (6156), 341–344.
- [9] Tan, Z.; Moghaddam, R. S.; Lai, M. L.; Docampo, P.; Higler, R.; Deschler, F.; Price, M.; Sadhanala, A.; Pazos, L. M.; Credgington, D.; et al. Bright Light-Emitting Diodes Based On Organometal Halide Perovskite. *Nat. Nanotechnol.* 2014, 9 (9), 687–692.
- [10] Lin, Jia; Chen, Hong; Gao, Yang; Cai, Yao; Jin, Jianbo; Etman, Ahmed S.; Kang, Joohoon; Lei, Teng; Lin, Zhenni; Folgueras, Maria C.; Quan, Li Na; Kong, Qiao; Sherburne, Matthew; Asta, Mark; Sun, Junliang; Toney, Michael F.; Wu, Junqiao; Yang, Peidong (2019). Pressure- Induced semiconductor-to-metal phase transition of a charge-ordered Indium halide Perovskite. *Proceedings of the National Academy of Sciences*, 116(47), 23404–23409. doi:10.1073/pnas.1907576116.
- [11] C.R. Kalaiselvi, N. Muthukumarasamy, Dhayalan Velauthapillai, Misook Kang, T.S. Senthil (15 May 2018). Importance of halide perovskites for next generation solar cells. <https://doi.org/10.1016/j.matlet.2018.02.089>
- [12] K. Capelle. A bird's-eye view of density-functional theory. ar Xiv:cond-mat, 0211443v5, 2006.
- [13] W. Koch and M.C. Holthausen. *A Chemists's Guide to Density Functional Theory*. Wiley-VCH, 2001.
- [14] W. Kohn. Nobel lecture: Electronic structure of matter - wave functions and density Functional. *Reviews of Modern Physics*, 71:12531266, 1999.

- [15] D.J. Gri-ths. Introduction to Quantum Mechanics. Pearson, 2005.
- [16] W. Kohn and L.J. Sham. Self-consistent equations include exchange and correlation Effects. *Physical Review*, 140:A1133A1138, 1965.
- [17] Karlheinz Schwarz. DFT calculations of solids with LAPW and WIEN2k. *Journal of Solid State Chemistry*, 176:319–328, 2003.
- [18] V.P. Gupta. Principles and applications of quantum chemistry. Academic press, 2016.
- [19] E. Schrödinger. An undulatory theory of the mechanics of atoms and molecules. *Physical Review*, 28:1049–1070, 1926.
- [20] F. Schwabl. *Quantenmechanik: Eine einfhrung (German)*. Springer, 2007.
- [21] D.J. Griffiths. Introduction to Quantum Mechanics. Pearson, 2005.
- [22] M. Born. On the quantum mechanics of collision processes (german). *Zeitschrift fuer Physik*, 37:863–867, 1926.
- [23] W. Koch and M.C. Holthausen. *A chemists’s guide to density functional theory*. Wiley-VCH, 2001
- [24] W. Pauli. The connection between spin and statistics. *Phys. Rev.*, 58:716–722, 1940.
- [25] A. Jabs. Connecting spin and statistics in quantum mechanics. *Found. Phys.*, 40:776–792, 2010.
- [26] W. Pauli. On the connexion between the completion of electron groups in an atom with The Complex structure of spectra. *Zeitschrift Physik*, 31:765, 1925.
- [27] N. Zettili. *Quantum mechanics: Concepts and applications*. Wiley-VCH, 2009.
- [28] K. Capelle. A bird’s-eye view of density-functional theory. *arXiv:cond-mat*, 2006.
- [29] D.A. McQuarrie and J.D. Simon. *Physical Chemistry: A Molecular Approach*. University Sciency Books, 1997.

- [30] M. Born and R. Oppenheimer. On the quantum theory of molecules (german). *Annalen Der Physik*, 389:457–484, 1927.
- [31] T. Fließbach. *Mechanik: Lehrbuch zur theoretischen physik I* (german). Spektrum, 2009.
- [32] P.A.M. Dirac. A new notation for quantum mechanics. *Mathematical Proceedings of Cambridge Philosophical Society*, 35:416–418, 1939.
- [33] C.B. Lang and N. Pucker. *Mathematische methoden in der physik* (german). Spektrum, 2005.
- [34] W. Koch and M.C. Holthausen. *A Chemists's Guide to Density Functional Theory*. Wiley-VCH, 2001.
- [35] A. Szabo and N.S. Ostlund. *Modern Quantum Chemistry*. McGraw-Hill, 1989.
- [36] W. Kohn. Nobel lecture: Electronic structure of matter - wave functions and density Functionals. *Reviews of Modern Physics*, 71:12531266, 1999.
- [37] P.O. Löwdin. Scaling problem, virial theorem and connected relations in quantum Mechanics. *Journal of Molecular Spectroscopy*, 3:4666, 1959.
- [38] M. Odelius and I. Josefsson. *Quantum chemistry - lecture notes*, 2009.
- [39] Frank Jensen. *Introduction to Computational Chemistry*. John Wiley & Sons, Ltd., 2007.
- [40] Zhiping Yin. Microscopic mechanisms of magnetism and superconductivity studied From First principle calculations. Pages 7, 8, 2009.
- [41] P. Hohenberg and W. Kohn. Inhomogeneous electron gas. *Physical Review*, 136:B864B871,1964.
- [42] A. Berger. *Current-Density Functional in Extended Systems*. PhD thesis, Rijksuni-Versiteit Groningen, 2006.

- [43] W. Kohn. Proceedings of the International School of Physics "Enrico Fermi", LXXXIX: 4pp, 1985.
- [44] Nathan Argaman and Guy Makov. Density functional theory-an introduction. American Journal of Physics, 1998.
- [45] Zenebe Assefa Tsegaye. Density functional theory studies of electronic and optical properties Of ZnS alloyed with Mn and Cr. Condensed Matter Physics, pages 11–13, 2012.
- [46] Errol G. Lewars. Computational Chemistry: Introduction to the Theory and Applications of Molecular and Quantum Mechanics. Springer, 2010.
- [47] Kh. Kabita and B. Indrajit Sharma. First principles study on structural, phase transition and Electronic structure of zinc sulfide ZnS within LDA, GGA and mBJ potential. Journal of Physics, 2016.
- [48] L. Mehdaouia, R. Miloua, M. Khadraoui, M.O. Bensaid, D. Abdelkader, F. Chiker, A. Bouzidi, Phys. B Condens. Matter 564 (2019) 114–124.
- [49] D. Jain, S. Chaube, P. Khullar, S.G. Srinivasan, B. Rai, Phys. Chem. Chem. Phys. 21 (2019) 19423–19436.
- [50] K. Benyahia, S. Bouchikhi, S. Bekhechi, Phys. Sci. Biophys. Journal 3 (2019) 1–6.
- [51] Tatu Ra janiemi. Electronic and optical properties of TiO₂ nanoclusters. 2016.
- [52] Javad Mousavi and M.R. Abolhasani. Calculation of the structural, electrical, and optical Properties of κ -Al₂O₃ by density functional theory. Journal of Physics, 2008.
- [53] Keith M. Glassford and James R. Chelikowsky. Structural and electronic properties of Titanium dioxide. Physical Review B, 46, 1992.
- [54] D.R. Penn, Phys. Rev. 128 (1962) 2093–2097.
- [55] A.S. Olayinka and W. Nwankwo. Comparative study of DFT and DFT-D methods for Electronic and optical properties of zinc-blende zinc sulfide (zb-ZnS). 9, 2019.

- [56] Hamza El Kouch Jamal Sayah, Larbi El Farh and Allal Challioui. Electronic and Optical Properties of Ramsdellite TiO₂ through mBJ Potential. *International Journal of Nanoelectronics and Materials*, 11:25–32, 2018.
- [57] M. R. Abolhassani S. J. Mousavi, S. M. Hosseini and S. A. Sebt. Calculation of the Structural, electrical and optical properties of κ -Al₂O₃ by density functional theory.
- [58] A. O. Isyaku, “Structural, Electronic and Optical Properties of Cu₂Sns₃ Solar Absorber: A First-Principle Density Functional Theory Investigation,” 2019, [Online]. Available: <http://repository.aust.edu.ng/xmlui/handle/123456789/4937>. *Chinese Journal of Physics*, 46, 2008.
- [59] M. Roknuzzaman, K. Ostrikov, K.C. Wasalathilake, C. Yan, H. Wang, T. Tesfamichael, *Org. Electron.* 59 (2018) 99–106.
- [60] A. Shukla, V.K. Sharma, S.K. Gupta, A.S. Verma, *Mater. Res. Express* 6 (2019) 126323.